Flood Risk of Embanked Areas and Potential Use of Dredge Spoils as Mitigation Measures in the Southwest Region of the Ganges-Brahmaputra-Meghna Delta, Bangladesh

Leslie Valentine¹
Department of Geology and Geophysics, Louisiana State University, Baton Rouge, LA, USA

Carol A. Wilson
Department of Geology and Geophysics, Louisiana State University, Baton Rouge, LA, USA

Md. Munsur Rahman
Institute of Water and Flood Management, Bangladesh University of Engineering and Technology, Dhaka, Bangladesh

Author accepted copy of manuscript. Suggested citation:

Valentine, L., Wilson, C. A., & Rahman, M. M. (2022). Flood risk of embanked areas and potential use of dredge spoils as mitigation measures in the southwest region of the Ganges—Brahmaputra—Meghna Delta, Bangladesh. *Earth Surface Processes and Landforms*, 47(4), 1073-1088.

Correspondence should be directed to Leslie Valentine, Department of Geology and Geophysics, Louisiana State University, Baton Rouge, LA 70802, USA. lvalen7@lsu.edu

2

3

Flood Risk of Embanked Areas and Potential Use of Dredge Spoils as

Mitigation Measures in the Southwest Region of the Ganges-

Brahmaputra-Meghna Delta, Bangladesh

4 Abstract

- In the 1960s, earthen embankments, locally known as polders, were first
- 6 constructed in the Ganges-Brahmaputra-Meghna (GBM) delta with the
- 7 intention of protecting agricultural lands from salinity; however, unintended
- 8 consequences of the barriers negatively impact the region. Once-active
- 9 distributary channels have morphed into terminal, headless tidal channels as
- the sediment-laden water that was once dispersed across the tidal deltaplain
- is now restricted by embankments. Elevation loss within embankments and
- channel siltation adjacent to embankments are deleterious consequences of
- hard engineering and pose significant flood risk when effective sea level rise
- is considered. The purpose of this study is to assess the current and future
- 15 flood risks of the embanked areas in the southwest region of the GBM delta
- and to expand on the potential for local-based solutions (e.g., mud plinths
- and embankments). We propose a novel source of material for these
- 18 structures—repurposed dredge spoils.
- 19 Project sites are along terminal tidal channels proximal to coastal towns in
- 20 the southwest region of the delta. We calculate here as the effective sea
- level rise will continue to increase in the years to come, the flood risk will

correspondingly increase (>67%). Geospatial analyses reveal several 22 23 prominent tidal channels have reduced in width over the last 30+ years, and recent dredging operations removed $\sim 1.7 \times 10^6 \,\mathrm{m}^3$ of sediment infill. Using 24 conservative values, we estimate the dredge spoils could be used to elevate ~20,000 houses on mud plinths or raise 18 km of existing embankments. On 26 27 a delta-wide scale, if all infilled tidal channels were dredged to 10% of their original widths, ~547,000 houses could be raised above the flood levels and 28 ~500 km of embankments could be elevated. With a mean household 29 population of 4.3 people, repurposing dredge spoils can positively impact 30 ~2.4 million people within the vulnerable SW region of the GBM delta. 31

32

33

25

- Keywords: deltas, poldering, dredge spoils, tidal channel siltation,
- effective sea level rise 34

1. Introduction

Earthen embankments are employed worldwide in deltaic regions to 36 protect surrounding lands from fluvial and tidal flooding, salinity incursion, 37 and storm surges (James P. M. Syvitski et al., 2009). While the 38 embankments provide a layer of defense, the lack of sediment input from 39 fluvial and tidal processes and subsequent subsidence of the embanked land 40 (locally called 'polder') poses a significant flood risk during prolonged 41 precipitation events or if the embankments fail (James P. M. Syvitski et al., 42 2009; Meade and Moody, 2010; Wang et al., 2012; Smajgl et al., 2015). 43 The embanked southwest region of the Ganges-Brahmaputra-Meghna (GBM) 44 delta is particularly vulnerable to catastrophic flooding, as the embanked 45 lands have lost an estimated 1-1.5 m in elevation since the construction of 46 the polders (Alam, 1996; Pethick and Orford, 2013; Auerbach et al., 2015). 47 Overbank flooding during high tides and storm surges previously distributed 48 sediment throughout the tidal deltaplain, but the embankments have 49 restricted new sediment deposition to unembanked lands and tidal channels 50 (Alam, 1996; Auerbach et al., 2015). Furthermore, accelerated compaction 51 and subsidence within the polders has taken place as mangrove forests were 52 cleared and farming practices involve the seasonal drying of agricultural 53 fields (Auerbach et al., 2015). Widespread siltation within the tidal channels 54 (>600 km to date; 90km²) blocks sluice gates, further exacerbating flooding 55

- and waterlogging within the polders (Alam, 1996; Rahman *et al.*, 2013;
- 57 Brammer, 2014; Auerbach *et al.*, 2015; Wilson *et al.*, 2017).
- Compounding this flood risk, tides amplify as much as 1-2.5 m as they
 propagate inland through the poldered regions (Pethick and Orford, 2013;
 Wilson *et al.*, 2017). Previously, flood risk in the GBM delta was assessed
 using the relative mean sea level (RMSL), which takes the average of
 measured high and low water levels. However, a study by Pethick and Orford
 (2013) showed this does not include tidal amplification. They thus quantified
 that effective sea level rise (ESLR) is more applicable to the region:
- 65 Eq. 1 ESLR = TA + Sb + Eu + FwQ
- where TA is tidal amplification, Sb is land subsidence (caused by a myriad of 66 factors, e.g., compaction, dewatering, fluid withdrawal, organic biomass 67 degradation), Eu is eustatic sea level change rate, and FwQ is fresh water 68 input (Pethick and Orford, 2013). ESLR highlights the trend of increasing 69 high water maxima (as TA increases), providing a more accurate evaluation 70 of flood risk in the SW embanked regions of the GBM where embankments 71 could be overtopped or breached by mesoscale tides or periodic storm 72 surges. In particular, (Pethick and Orford, 2013) found the RMSL rise 73 74 decreases from the coast to Khulna, 120 km inland (from 7.9 to 2.8 mm a 1), while the ESLR rate (Eq. 1) increases significantly (from 10.7 to 17.2 mm 75 a⁻¹). In addition to excluding ESLR, many flood risk assessments are based 76

on the original Shuttle Radar Topography Mission (SRTM) digital elevation models (DEMs) originally collected in 2000, meaning that 20 years of subsidence of embanked regions (and likewise accretion in the unembanked regions) is unaccounted for. Additionally, the original SRTM data did not remove vegetation cover, thus tree-lined roads look exaggerated compared to rice paddies and aquaculture ponds. The CoastalDEM re-processing of this data (shown in Fig 1;(Kulp and Strauss, 2019)) attempted to better remove this vegetation cover, providing more accurate elevations, however for a survey conducted now decades ago.

Channel siltation within the GBM delta not only affects the flooding potential of the polders but also blocks waterway traffic, a main mode of transportation (Rahman *et al.*, 2013). The most common solution is a combination of hydraulic and mechanical dredging, where the infilled material is excavated and placed alongside the channel margins (Rahman *et al.*, 2013; Hossain, Khan and Shum, 2015; Sultana, Uddin and Analysis, 2017). Over the next 50 years, the Bangladesh Inland Water Transport Authority (BIWTA) plans to dredge 178 rivers (> 10,000 km) to ensure navigability (The Daily Star, 2020). While efforts are underway to implement large scale dredging operations, small-scale sediment redistribution efforts are also recommended to ameliorate elevation deficits in embanked areas by flushing sediment from tidal channels (a practice locally called Tidal River Management; Shampa and Pramanik, 2012; Amir *et al.*, 2013; Gain *et al.*,

2017). Mitigation for flood risk requires data-driven investigations on the effectiveness and feasibility of these different methods, and incorporation of accurate, up-to-date information.

This study combines established ESLR rates with newer, high resolution (<20 mm accuracy) elevation data obtained with a Leica GNSS unit and relates these elevations to measured local tidal water fluctuations to provide a more accurate flood assessment of the study region. We assess the sedimentological properties of unembanked and embanked regions to characterize the sedimentary deposits where tides still distribute sediment and where they are precluded, respectively. Finally, we quantify how much sediment is removed from tidal channels during recent dredging practices and make suggestions for the repurposing of this dredge material in line with common practices for this delta and other deltas worldwide.

2. Study Area

The tidal-dominated landscape of the GBM delta experiences semi-diurnal mesoscale (2-4 m) tides. In the 1960s, the Bangladesh government began constructing earthen embankments to protect agricultural land from salinity incursion, and the land within the embankments are referred to as polders (Allison and Kepple, 2001; Bricheno, Wolf and Islam, 2016; Ayers *et al.*, 2017; Bomer, Wilson and Datta, 2019). While the embankments provide a layer of protection, elevation surveys of Polder 32 from Auerbach et al. (2015), revealed embanked elevations were 1.0-1.5 m below adjacent

122

123

124

125

126

127

128

129

130

131

132

133

134

135

136

137

138

139

140

141

142

unembanked elevations in the Sundarbans, the world's largest mangrove preserve (Fig. 1). The elevation data collected from Polder 32, combined with SRTM data, was then extrapolated deltawide to assess flood risk. However, the applicability of the data in calculating present-day and future flood risk is limited due to the outdated SRTM data.

The Baleswari River demarcates the boundary between the tidaldominated and fluvio-tidal dominated landscapes (Fig. 1), with the fluviotidal region receiving year-round fluvial input from the Lower Meghna River on the scale of 50,000-100,000 m³/s during the monsoon season to 5,000-30,000 m³/s during the dry season (EGIS, 2000; Whitehead et al., 2015). Tides dominate in the western region as discharge from the main source of fluvial input, the Gorai River (a distributary of the Ganges), has decreased 40% over the past 50 years – from an average monsoonal discharge of 5,500 m³/s to 3,000 m³/s and an average dry season discharge waning from 2900 m³/s to <1000 m³/s (Mirza, 1998; EGIS, 2000; Pethick and Orford, 2013). The decrease in discharge along the Gorai is often attributed to the construction of the Farraka Barrage along the Ganges River in India, but the morphology of the offtake angle of the Gorai River is likely another significant contributing factor (Mirza, 1998; Winterwerp and Giardino, 2012). As the Gorai River approaches the Bay of Bengal, elevation and fluvial flow velocities decrease, and the river divides into a network of distributary tidal channels, including the Pussur, Sibsa, and Baleswari Rivers (Fig. 1) that

receive most of their water through bi-directional tidal currents that propagate >100 km inland from the Bay of Bengal.

143

144

145

146

147

148

149

150

151

152

153

154

155

156

157

158

159

160

161

162

163

164

The Pussur and Sibsa Rivers are two of several high order channels in the tidal-dominated SW region of the GBM delta (Fig. 1), connected ~60 km upstream from the coast by a series of transverse conduit channels, and both have an estimated net tidal prism (m³) on the scale of $\approx 10^7$, (Bain, Hale and Goodbred, 2019; Hale et al., 2019). Previous research has shown that poldering in the SW region of the delta near these two tidal rivers has caused numerous smaller order channels to become "dead end" and infill as the tidal prism is reduced; many have to be dredged periodically to maintain navigability (Rahman et al., 2013; Wilson et al., 2017). For this study, we focus on three representative second-order tidal channels (average width <300 m) that stem from the Pussur channel (locally called Rupsa River) near the cities of Khulna, Dacope, and Rampal, and the surrounding embanked areas (Fig. 1). All three channels are bounded by embankments and have infilled over the past 35+ years, and subsequently been dredged within the last ten years with dredge spoils deposited along the margins (Fig. 2). Combining our elevation surveys with local tide data allows for flood risk assessments of the unembanked and embanked areas adjacent to the tidal channels. By calculating rough estimates for channel water and sediment volumes for three representative tidal channels in the lower deltaplain, we can quantify how tidal channels and adjacent land surface elevations are

evolving under natural and anthropogenic forces and how much sediment has been historically dredged from these channels.

3. Methods

3.1. Elevation measurements and relationship to tidal water level datums

Elevation transects were measured (relative to elevation datum EGM 96) using an RTK (real-time kinematic) GPS system with a Leica GS36 base antenna and GS38T rover. Leica GS38T has tilt compensation with <20 mm accuracy (tilt angle <30°). When surveying an area, a general grid pattern with perpendicular transects was generated, and the rover automatically measured point data (X, Y, Z) every 3 m. Extensive aquaculture ponding posed a challenge to obtain large-scale, contiguous surveys at all locations except for the Khulna outside embankment ("Khulna_out_"); thus, multiple small-scale surveys were conducted at the other sites. Once the points were measured, elevation profiles were created using kriging interpolation in Surfer 17®. Studies have shown kriging is useful in small areas as it distributes weight based on statistical autocorrelation, and the result is a smoother grid/3D surface than that of other commonly used interpolation methods (e.g., nearest neighbor or bilinear (Arun, 2013)).

To obtain the water surface elevations relative to EGM 96, HOBO® pressure sensors were deployed at locations that received tidal input, then water surface elevations (relative to EGM 96) were measured with the Leica GPS system from the shoreline, noting the time. The water surface

measurements taken with the Leica GNSS system were cross-referenced with the relative water surface elevations (HOBO®) to calculate absolute water surface levels at different tidal stages relative to EGM 96. It was necessary to obtain water surface elevations in the EGM 96 datum to compare the values to those from local tide datums (i.e., the Bangladesh Public Works Datum [PWD] or individual tide gauge Chart Datum), as no clear relationship currently exists between the three datums. This is especially important when assessing the flood risks of the study areas by comparing elevation data (in EGM 96) to predicted ESLR rates (which is currently in PWD; see Supplemental Section 2 for more details).

3.2 Coring and Sedimentological Analyses

In-depth sediment analyses are pertinent to this study as bulk density, grain size, and organic mass content provide the necessary information to understand the elevation dynamics and accurately estimate the volume of dredge spoils that are needed for the two repurposing methods – constructing plinths and elevating existing embankments. Sediments were characterized in two focus areas of 12 cores extracted in October 2019 (Fig. 3). Core locations were chosen based on infilling observed in historical imagery (1984-present). All twelve cores were extracted along the representative terminal tidal channels shown in Figure 1; six cores were extracted outside the embankments and the other six cores were extracted inside the embankments (Fig. 3). Two coring methods were utilized for this

project – auger coring and vibracoring—to achieve maximum penetration and recovery. Auger cores were extracted by hand using a 5.08-cm diameter Edelman combination auger to an average depth of 3.8 meters, subsampled in the field at 20 cm intervals. Compaction during auger coring is minimal. Vibracores were collected following the methods of Lanesky et al. (1979), using a 6 m section of 7.5-cm diameter aluminum pipe and cement vibrator. Vibracores were then taken to the Department of Environmental Science at Khulna University where they were split, photographed, and subsampled in 10 cm increments. Only 3 vibracores were analyzed due to high compaction and/or plugging in most locations. All core samples were then shipped and analyzed at Louisiana State University Sedimentology lab for bulk density, organic content via loss-on-ignition, and grain size detailed below.

Bulk Density

For each core, $\sim \! 10$ g of sediment was sampled every 20 cm using a 10 mL syringe to create a measured sample volume of sediment. Sediment wet mass was determined (m_w ; g) and samples were then dried in an oven at 60° C for 72 hours and reweighed to determine the dry mass (m_d). The dry mass was divided by the volume (v) of each sample to calculate the bulk density:

$$Eq. 2$$
 bulk density = m_d / v .

230 Loss-on-Ignition

Using the sediment subsamples from all cores, ~5-10 g of dried sediment was homogenized using a mortar and pestle, combusted in a muffle furnace at 550°C for 5 hours, and reweighed to yield weight loss on ignition. This method is commonly used to calculate percent organic matter from soil samples (Heiri et al., 2001; Hoogsteen et al., 2015):

236 Eq. 3 % organic matter =
$$\frac{m_b}{m_s} x 100$$

where m_b is the biomass and m_s is the sample mass before burning.

Grain-Size Analysis

Approximately 2 g of sediment (pre-combustion) from each subsample was placed into 50 mL centrifuge tubes, and ~2 ml of 30% hydrogen peroxide was mixed to oxidize organic matter. Then ~15 ml of 0.05% sodium metaphosphate was added to each test tube to deflocculate clay particles. Finally, the samples were run through a Beckman Coulter Laser Diffraction Particle Size Analyzer (Model LS 13 320) to calculate volumetric abundance of grain sizes from 0.37 to 2000 microns.

3.3 Channel Infilling Analyses and Geometric Calculations

Detailed channel infilling and erosion were analyzed using historical imagery in ArcMap 10.7.0 along with GIS-based geometric calculations.

Three moderately sized representative tidal channels that collectively span 60+ km in the lower tidal deltaplain were chosen for these analyses (Fig 1).

For years 1984-2010, LandSat imagery (resolution 30 meters) was used for

the analyses. For years 2010-2020, imagery procured from Google Earth and the Copernicus Open Access Hub with a much higher resolution of 2.5 meters were used. The images were cross-referenced with tide data to ensure all were representative of low tide stages – increasing the accuracy of the channel width measurements. Only tidal channels outside of polder embankment walls were analyzed because the resolution prior to 2010 was not fine enough to accurately map smaller channels within the embankments whose widths were <30 meters. While dredging was observed remotely and in person during field campaigns, detailed reports as to the exact locations and volumes of dredged sediment is not public information; therefore, dredge spoil volumes for the 3 channels are estimated through channel width measurements.

To measure channel width, channel centerlines were traced from the imagery using polylines for each year. Using the Channel Migration Toolbox in ArcMap, perpendicular transect lines were generated with 200 meter spacing starting at the mouth of each tidal channel. Each channel was then segmented into 100 transects, covering 20 continuous kilometers of the tidal channel. The channel widths were measured by hand at each transect. After 20 kilometers, the widths of several channels were too narrow to accurately measure in the LandSat images due to the lower resolutions. Measured channel widths were then used to calculate average channel depths using

the width:depth equation established in this delta region by Bain et al. (2019):

275 Eq. 4
$$d^* = 0.17 \times w^{*0.6}$$

where d* is channel depth and w* is channel width. This equation is applicable to tidal channels that are >10 km inland from the coast; as channels will shoal with proximity to the coast, depth calculations would be overestimated for channels <10 km from the Bay of Bengal (Bricheno, Wolf and Islam, 2016; Bain, Hale and Goodbred, 2019). The cross-sectional area of each transect was then calculated using the equation of a half-ellipsoid as this shape best represents overall channel geometry without involving intensive calculus formulas and was based on bathymetric profiles collected in local tidal channels (Rahman *et al.*, 2013; Auerbach *et al.*, 2015; Wilson *et al.*, 2017):

$$Eq. 5 CA = \frac{\frac{w}{2} \times d \times \pi}{2}$$

where w is the channel width, d is the channel depth calculated from Equation 4, and CA is the cross-sectional area of a transect. As the tidal prism is decreasing, the entirety of the channels is infilling from upstream to downstream. That is, the channel bed and flanks are simultaneously aggrading (Rahman *et al.*, 2013). Once cross-sectional areas were calculated, estimates of the volume of water between individual transects could be made using the following equation:

294 Eq. 6 Volume₁₋₂ =
$$\frac{l}{3} * (CA_1 + CA_2 + \sqrt{CA_1CA_2})$$

where / is the length between the two transects (=200 m), CA₁ and CA₂ are cross-sectional areas of the two transects, respectively. Subsequently, all inter-transect volumes are summed to calculate a total volume of the 20 km segment, which is an estimate of the tidal prism, or total volume of water accommodated over a tidal cycle (see Supplemental Section 5 for more details).

If a channel is infilling with sediment over time, it can be assumed/postulated that the volume of water within the channel will decrease. By subtracting the water volume of the channels before dredging from the respective channel's water volume of 1984, the amount of sediment deposition within the channels over time was calculated. If a channel is subsequently dredged, a significant amount of the infill material is removed and the channel water volume will increase. In this region, dredged material is typically deposited on either side of the channel, forming an artificial levee. Error for the volume estimates was calculated based on the same channel width measurements but different depths calculated from Eq 4, as this is the largest uncertainty (±1 m).

4. Results

4.1 Elevation Data

314	Table 1 compiles all site elevation data measured. In general, elevation
315	decreases with proximity to the coast, and sites outside of embankments
316	(designated nomenclature "_out_") are higher in elevation than sites within
317	embankments ("_in_") by at least 1 m. In particular, the Khulna_out_ sites
318	(~120 km from the Bay of Bengal coast) had an average elevation of 4.54 \pm
319	0.06 m compared to Khulna_in_ sites (2.86 \pm 0.04 m) (Table 1; Fig. 4).
320	Rampal_out_sites (~90 km from Bay of Bengal) had an average elevation
321	of 3.98 m \pm 0.09 m, while the corresponding Rampal_in_sites average
322	elevation was 2.91 ± 0.03 m (Table 1; Fig. 5). Typical elevation variability
323	with tidal river morphology outside of embankments was also observed: a
324	measured cutbank (Khulna_out_1) had an average height of 5.08 \pm 0.05 m
325	(ranging from 2.00 to 7.01 m), while the opposite point bar (Khulna_out_2
326	and Khulna_out_3) had a lower average elevation of 3.52 \pm 0.05 m (ranging
327	from 2.27 to 5.37 m; Table 1; Fig. 4). Note all of these elevations were
328	greater than the elevations within the embankment.
329	Water surface points (x, y, z) were combined with HOBO® sensor data to
330	calculate the absolute tide levels and compare to land surface elevation with
331	respect to EGM 96. Khulna_out_ sites were temporarily disconnected from
332	the tide as dredging was ongoing. While HOBO® pressure data was not
333	collected for the site, the water surface elevation was 2.0065 \pm 0.05 m
334	relative to EGM 96 during the field survey on October 26, 2019.

Alternatively, the Khulna_in_sites remain connected to the tides through a

335

337

338

339

340

341

342

343

344

345

346

347

348

349

350

351

352

353

354

355

356

357

sluice gate ~6.5 km downstream as evidenced by small tidal fluctuations (<0.2 m observed), but the water surface elevation measurements could not be cross-referenced with the HOBO® data as the two data sets were measured on different days. For the Rampal out sites, HOBO® data was collected over a 6 hour period, exhibiting a water surface elevation range of 1.126 m. This data was compared to predicted astronomical tide charts for Mongla, a nearby (~15 km) port city on the Pussur River (Fig. 5). The water surface elevation at Rampal at high tide during the survey period was calculated to be ~2.5 meters relative to EGM 96; this is 1.4 m below the average elevation of the Rampal out sites and only 0.4 m below the average elevation of the Rampal in sites (Fig. 5; Table 1). However, the predicted monthly Mean High Water (mMHW), the average of all tidal high water during spring and neap tides, is 3.5 m relative to EGM 96, which is still below the average elevation of the Rampal out sites but exceeds the average elevation of the Rampal in sites by 0.6 m (Fig. 5; Table 1).

4.2 Sedimentological and Stratigraphic Analyses

Figure 6 shows a representative core, a vibracore from an unembanked Rampal location, which is exemplary of all cores collected. The presence of tidalites and other small bedding structures such as flaser and lenticular bedding were visible in the vibracores (Fig. 6). Auger coring destroys such bedding, but small fluctuations in grain size are evidence of such tidal signatures. All cores were silt-dominated (named simply here as

"silt"), with median grain size ranging 11-55 μ m (6.5 to 4.2 Φ), averaging 32 μ m (5.0 Φ), and clay and sand grain sizes independently comprising <25% of the substrate. Shepard's diagram was used to determine the nomenclature ("silt", "sandy silt", "clayey silt") of each sample (Shepard, 1954). All the cores had multiple sandy silt beds, ranging in thickness from 10 to 260 cm, averaging 45 cm. Only one sample of clayey silt was present in all the cores (Rampal out 3 core at a depth of ~260-270 cm). Bulk densities for all sites, embanked and non-embanked, ranged from 1-1.8 g/cm³, with an average of 1.4 ± 0.2 g/cm³. Organic content for every core averaged <5%. In figure 4, all the cores from the Khulna sites are plotted with their respective elevations (relative to EGM 96) – the embanked sites having a much lower average elevation of 2.86 ± 0.04 m compared to that of the unembanked sites 4.54 ± 0.06 m (Table 1). The unembanked Khulna sites also have more sandy silt beds near the surface, indicative of hydrologic connectivity to the tides. The elevations for the embanked and unembanked Rampal sites also offset from each other by ~1 m, and the stratigraphy closely resembles the Khulna sites – sandy silts at depth with finer silts near the surface. All core logs, including stratigraphy, lithology, median grain size, bulk density, and organic content can be viewed Section 3 of the Supplemental.

4.3 Channel Infilling Rates

358

359

360

361

362

363

364

365

366

367

368

369

370

371

372

373

374

375

376

377

378

Between 1984 and 2020, average channel width decreased 39%, 87%, and 72% for Khulna, Dacope, and Rampal channels, respectively. Detailed graphs of channel width variability are available and described in the Section 5 of the Supplemental. In general, average channel width decreased most notably in the upstream reaches (>10 km upstream from channel mouth). It is evident from aerial imagery that all 3 channels were extensively dredged between 2010 and 2020.

Figure 7 and Table 2 quantify the water volume accommodated in the 3 representative channels from 1984 to 2020, including notation when dredge operations began and completed. Dacope experienced the most infilling, with water volume of 16.2×10^6 m³ in 1984 to 0.39×10^6 m³ in 2012 before dredging, a 97% reduction (Fig. 7). From 1984 until dredging, Khulna and Rampal experienced reduction in water volumes of 47% and 93%, respectively (Fig. 7). From these measurements, there was a cumulative deposition of 24.2×10^6 m³ of sediment for all three channels between 1984 and 2010 (Table 2). All three channels were subsequently dredged, but the channels were not dredged to their original widths (original widths averaged ~ 165 m, dredged widths averaged ~ 52 m). As a result, we calculate a total of 1.7×10^6 m³ of sediment was removed by dredging operations in these three channels between 2010 and 2020 (Table 2).

5. Discussion

5.1 Elevation and Hydrologic Connectivity Controls on Sedimentation

401

402

403

404

405

406

407

408

409

410

411

412

413

414

415

416

417

418

419

420

421

422

The coastal zone of Bangladesh has been identified as one of the world's most vulnerable "sinking" deltas as much of the region is subsiding and susceptible to tides, storm surges, and relative sea level rise (James P. M. Syvitski et al., 2009). The embanked regions are particularly vulnerable as the polders preclude sediment exchange from the tides, greatly reducing sediment input that would otherwise increase the relative elevation (James P. M. Syvitski et al., 2009; Auerbach et al., 2015; Dunn et al., 2019). This trend is seen among the Khulna and Rampal sites – the average elevations outside of the embankments are greater than the elevations of embanked regions by 1-1.5 m (Table 1; Fig. 4), which aligns with previously estimated elevation loss within embankments in the southwest region of Bangladesh (Auerbach et al., 2015). This means that embanked landscapes are particularly vulnerable to flooding and storm surges, as evidenced by breaching and subsequent flooding of Polder 32 by Cyclone Aila in 2009 (Auerbach et al., 2015) and more recent catastrophic breaches in the southwest from Cyclone Amphan in 2020 (Khan et al., 2020).

Deltas across the world are experiencing natural tidal amplification as a byproduct of sea level rise (Holleman and Stacey, 2014), and polders compound the problem of tidal amplification by having a funneling effect. That is, the tides that once flooded the delta plain are now forced to flow through a much smaller area outside embankments. Pethick and Orford

424

425

426

427

428

429

430

431

432

433

434

435

436

437

438

439

440

441

442

443

444

(2013), note that the Relative Mean Sea Level (RMSL, an average of the hourly sea level over months or years) at Hiron Point, a coastal area directly south of the study area, is increasing at a rate of 8.8 mm/yr. Meanwhile, ~120 km inland near Khulna, the RMSL is only increasing by 2.8 mm/yr. They determined this does not reflect the actual effect of tidal amplification, opting to calculate the Effective Sea Level Rise (ESLR) instead. The ESLR at the coast is 10.9 mm/yr (greater than the 8.8 mm/yr RMSL rise), and inland sites near Rampal and Khulna are at much greater risk with ESLR rates of 14.5 mm/yr and 17.2 mm/yr, respectively (Pethick and Orford, 2013). This is a serious threat to all coastal regions, but especially embanked regions as their average elevations are often more than 1 m below surrounding unembanked areas (this study; Auerbach et al., 2015). With ESLR, the embankments are more important than ever as much of the poldered landscape is below the mMHW (the monthly Mean High Water, which is the average of all tidal high water during spring and neap tides) – meaning that without embankments, the landscape would flood multiple times every year, sometimes multiple times a day (Fig. 5B).

We compare our measured elevation data of embanked and unembanked regions to the ESLR measured by Pethick and Orford (2013) to assess current and future flood risk of embanked regions in SW Bangladesh. Pethick and Orford (2013) detail the monthly mean high water, mMHW, for the region, but they used a local datum—PWD (Public Works Datum)—

instead of EGM 96. We determined that updated elevation data measured in this study (in EGM 96) can be converted to PWD with the following equation (see Supplemental Section 2 for conversion information): 447

448 Eq. 7 PWD (m) = EGM 96 (m)
$$- 0.48$$
 m

The predicted mMHW water levels in Khulna from Pethick and Orford (2013), 449

450 Eq. 8
$$y = 0.0172x - 32.02$$

445

446

451

452

453

454

455

456

457

458

459

460

461

462

463

464

can be used to calculate the year (x coefficient) in which the mMHW (y coefficient) has/will exceed the average embanked elevations. If y, in this case, is the average embanked elevation we measured at our Khulna sites (located ~ 8 km east of the Khulna tide gauge = 2.86 m EGM 96), we can convert this elevation to PWD (using Eq. 7: 2.86 m EGM 96 - 0.48 m = 2.38m PWD), then plug into Eq. 8: 2.38 = 0.0172x - 32.02. Solving for x, we calculate the mMHW surpassed the average elevation of embanked locations near Khulna in 2000. Tidal data from BIWTA reveals that the maximum daily water level never exceeded the embanked elevations from 1996 through 2010, except for 6 days in total. However, from 2013 to 2016, the maximum daily water level surpassed 2.86 m (relative to EGM 96) an average of 30x each year. Pethick and Orford (2013) also provide an equation for the estimated rate for increase in mMHW in Mongla, which is 20 km southwest of our Rampal sites on the Pussur River:

465 Eq. 9
$$y = 0.0145x - 26.252$$

Given the proximity to Rampal as well as the synchronous tides (Fig. 5A), the estimate for Mongla is applicable to the Rampal study area. Using the average embanked elevation of Rampal (2.91 m EGM 96 = 2.43 m PWD) to solve for x, mMHW in Rampal exceeded the embanked elevations over 40 years ago in 1978. Since 2011, the maximum daily water level has exceeded the embanked elevation an average of 58x each year, and the frequency in which this occurs is increasing over time (Fig. 5B).

Figure 8 shows that monthly MHW (mMHW) near Khulna and Rampal consistently exceed the average embanked elevations in these regions of the tidal deltaplain. Furthermore, we show this trend will increase in magnitude over the next 30 years with measured rates of ESLR from Pethick and Orford (2013), with inundation depth increasing from 0.3 at present to 0.9 m by 2050 at Khulna, and from 0.6 to 1 m at Rampal – increases of 200% and 67%, respectively (Fig. 8). As such, we show the area will become progressively more vulnerable to catastrophic flooding if an embankment wall fails during times of high water level. By comparison, unembanked regions near Khulna and Rampal appear to have kept pace with measured rates of ESLR (Fig. 8). Similar elevation pacing has been observed on unembanked regions along riverbank terraces southwest of Mongla (Auerbach *et al.*, 2015) and in the Sundarbans (Bomer *et al.*, 2020). Our results highlight the critical importance of sediment delivery to maintaining

elevation in the face of ESLR in this delta, and without mitigation measures, flood risk will significantly rise over the next 30 years.

487

488

489

490

491

492

493

494

495

496

497

498

499

500

501

502

503

504

505

506

507

508

While elevation surveys performed here corroborate with previous work that emphasizes the elevation loss in poldered vs non-poldered landscapes due to the loss of hydrologic connectivity (e.g. Auerbach et al., 2015; Bomer et al., 2020; Hossain et al., 2015), the stratigraphy and lithology of poldered lands is also elucidated. Our results corroborate with previous data from cores extracted from an infilled tidal channel near Dacope (outside embankment), displaying similar silt-dominated tidal signatures, with an overall fining upward sequence (Chamberlain et al., 2017; Wilson et al., 2017), but we provide new data from cores extracted within embankments for comparison. With hydrologic disconnect, finer sediment deposition (silts, clays, and organic rich sediment) at the embanked sites is expected due to a reduced tidal prism and subsequent decrease in tidal velocities (Hesselink, Weerts and Berendsen, 2003; Davis and Dalrymple, 2011). This correlates with the predominance of silt in the top meter of cores from embanked sites (Fig. 4; see also Supplemental figures S4 and S5). All Khulna out cores are dominated by sandy silt in the top meter, while all Khulna in cores are dominated by finer-grained silt layers. The grain-size difference in the top meter of all Rampal cores is less noticeable, but there is a general fining of sediment between what is deposited outside vs inside embankments: Rampal out 1 and 3 are capped

510

511

512

513

514

515

516

517

518

519

520

521

522

523

524

525

526

527

528

529

530

by sandy silt beds, while Rampal_out_2 and all Rampal_in_ cores are capped by silt beds. At depth, all cores have sandy silt and silt beds, with tidal signatures evidenced by tidalites and fluctuating fine-grain size (Fig. 6 and S6, S7, S8, and S9). Since all cores are silt-dominated and representative of the study region, we can assume that the sediment throughout the SW of the GBM delta dewaters and compacts with time, creating accommodation space due to the high porosity of silts and clays as well as their flat, platy mineralogic structure which allows for great compaction (Meckel, Ten Brink and Williams, 2007; Duncan, Wright and Brandon, 2014; Brain, 2016). The unembanked sites, which are hydrologically connected to diurnal mesoscale tides, receive new sediment that fills this accommodation space and even keeps pace with ESLR (Fig. 8; Bomer et al., 2020). However, the embanked sites (i.e. polders) have gained little to no elevation since being hydrologically disconnected from the tides, leaving its land and inhabitants increasingly vulnerable to flooding should an embankment fail (Fig 8; (Syvitski et al., 2009; Auerbach et al., 2015; Wilson et al., 2017). While the unembanked regions can keep pace with ESLR, there is excessive sedimentation in the tidal channels, compounding the waterlogging problem.

5.2 Channel Infilling and Dredge Spoil Repurposing

Over the past 50+ years, tidal channels adjacent to and within embankments have been rapidly infilling, effectively blocking navigation (Wilcox, 1930; Mukerjee, 1938; Majumdar, 1941; Alam, 1996; Rahman et

535

536

537

538

541

549

551

al., 2013; Brammer, 2014; Chamberlain et al., 2017; Wilson et al., 2017). 531 532 The widely accepted solution to this problem is channel dredging, and Bangladesh has begun to implement a master-plan that will ultimately 533 dredge 178 major rivers throughout the country in the next 50 years (The Daily Star, 2020). However, we show here that with mechanical dredging in the southwest region of Bangladesh: (1) the 2nd and 3rd order channels are only dredged to ~10% of their original widths (Fig. 3) – just enough to allow waterway traffic, and (2) the dredge spoils are often disposed alongside the dredged channels, forming an artificial levee outside the embankment walls 539 (Figs. 2 & 4). Rahman et al. (2013) detail the infilling, dredging, and 540 subsequent backfilling of the Mongla-Ghasiakhali route, a significant navigation channel. The study concluded that dredged tidal channels will 542 rapidly backfill, especially during the dry season due to tidal pumping and 543 decreased fluvial velocities (Rahman et al., 2013). We propose that instead 544 of discarding dredge spoils along channel margins, dredge material should 545 be removed and repurposed, preferably for flood mitigation purposes in this 546 flood-prone region of the delta. This material could be used to: (1) elevate 547 houses and/or (2) elevate existing embankment walls (Fig. 9). Repurposing 548 the dredged material would not only mitigate the rapid backfilling by moving the sediment away from the channel but also provide added protection to 550 local people from elevation deficits and enhanced flood risk with ESLR. Both repurposing methods are widely used throughout the GBM delta, with over 552

554

555

556

557

558

559

560

561

562

563

564

565

566

567

568

569

570

571

572

573

US\$220 million going towards the rehabilitation and improvement of existing polders in the Coastal Embankment Improvement Project (CEIP), funded by World Bank (Arifuzzaman and Zaman, 2013; BWDB, 2013). Thus, we are not introducing foreign mitigation measures but instead embracing local flood solutions.

As much of the GBM delta is prone to flooding and waterlogging, locals alleviate this problem by elevating their houses above the MHW on earthen foundations called plinths (Arifuzzaman and Zaman, 2013). If the dredge spoils from the three representative channels (total amount of sediment removed was 1.70 x 10⁶ m³; detailed in Table 2) is repurposed for elevating houses, we estimate 16,700-20,100 houses can be raised above the predicted mMHW for 2050 (calculations in Table S1 in Supplemental Material). This estimate was calculated using the following assumptions: (1) housing plinths are 7.5 m x 7.5 m x 1.5 m (average house size, local observations) and (2) dredge spoils have gone through the natural process of dewatering (consolidation) after excavation (Duncan et al., 2014) and (3) maximum secondary compaction of the dredge spoils is 20% (factor of 1.2; see Supplemental Section 4; Holtz, Kovacs and Sheahan, 1981). If little to no secondary compaction takes place, the total volume of a typical plinth is estimated to be 84.375 m³. However, with maximum secondary compaction the amount of sediment required to construct each plinth is 101.25 m³.

575

576

577

578

579

580

581

582

583

584

585

586

587

588

589

590

591

592

593

594

595

Alternatively, the dredge spoils can also be repurposed to maintain and elevate embankments. If the volume of available dredged sediments from the 3 study sites calculated here $(1.70 \times 10^6 \text{ m}^3)$ was used exclusively for raising embankments above predicted storm surges, 15-18 km length of embankments could be raised to a height of 6.8 m (calculations in Table S1 in Supplemental Material). This calculation was based on the dimensions for interior polders in the GBM delta tidal delta plain detailed by World Bank (Dasgupta et al., 2010) and proposed embankment elevations detailed by the Coastal Embankment Improvement Project (CEIP) – Phase I report (BWDB, 2010) and the Bangladesh Delta Plan 2100 (Rahman et al., 2019). The dimensions for the interior polders at present-day are as follows: a top base of 4.3 m, an average height of 3.8 m, and an average bottom base of 22.8 m (Fig. 9). Thus, to increase the height of a 1 km segment of embankment to 6.8 m while maintaining the slope ratios on the embanked (1:2) and unembanked (1:3) sides, an additional volume of 92,400 m³ of sediment is required. Factoring in a maximum estimate for secondary compaction as previously mentioned (=1.2x), this would equate to 110,880 m³ of sediment. It is important to note that while CEIP proposes increasing the embankment elevations, most embankment failures are not caused by overtopping from storm surges; rather it has been reported that the structural integrity of the embankments fail due to thrust forces during storm surges (Haque et al., 2019). Therefore, while embankments need to

597

598

599

600

601

602

603

604

605

606

607

608

609

610

611

612

613

614

615

616

617

be elevated to maintain elevation deficits caused by ESLR, the strength of the entire structure should be assessed.

While 16,700 housing plinths and 15 km length of embankments may not seem substantial, they only account for ~60 km length of channels reported here outside of embankments that have been recently dredged. Previously, Wilson et al. (2017) quantified that >600 km of tidal channels have silted in over the entire southwest GBM delta, and the volume of sediment contained within these infilled channels (locally called 'khas-land') is 462 x 10⁶ m³. From the aerial imagery analyses from this project, it is estimated that only 10% of the channel widths are dredged, i.e., the channels are not dredged to their original width, only to a width required to maintain vessel navigation. Thus, if we take these trends and extrapolate that further dredging could supply 10% of the 462 x 10⁶ m³ of sediment available for repurposing after dredging operations, this would result in 46.2 x 10⁶ m³ of sediment dredged – which could elevate 456,000 – 547,000 houses with mud plinths or elevate 415 - 500 km of embankments. With a mean household of 4.3 persons (Carrico et al., 2020), repurposing the dredge spoils can impact ~2.4 million people throughout the Ganges delta (nearly 35% of the population in the tidal deltaplain west of the Baleswari River).

5.3 Mitigating Flood Vulnerability - Dredge Spoil Repurposing vs.

Tidal River Management

Dredge spoil repurposing is not a novel idea, with many different uses proposed and employed in various deltas today (Ford, Cahoon and Lynch, 1999; Brandon and Price, 2007; Daniels, Whittecar and Carter, 2007; Allison and Meselhe, 2010; Sheehan and Harrington, 2012; Mao *et al.*, 2018; Baptist *et al.*, 2019). Much like other densely populated deltas, the Yellow River delta (YRD) is forced to cultivate salt-affected soils as demand for food increases with population and soil salinity increases with sea-level rise (Fan *et al.*, 2012; Dasgupta *et al.*, 2015; Daliakopoulos *et al.*, 2016). New studies suggest that dredged material – poorly graded sand – from the YRD can be mixed with the saline, clayey flood plain soils to improve agricultural productivity (Mao *et al.*, 2016, 2018). Additionally, YRD sediments are deposited on agricultural lands adjacent to underground coal mines to combat subsidence and reduce waterlogging (Duo and Hu, 2018).

Sediment redistribution is also used to attenuate subsidence in the Mississippi Delta (MD) of Louisiana where marshes and coastal wetlands are rapidly deteriorating from lack of sediment supply. Both anthropogenic and natural mechanisms contribute to regional subsidence in the MD (e.g., compaction of organic-rich Holocene sediments (Törnqvist *et al.*, 2008), sediment loading (Blum *et al.*, 2008), tectonics (Gagliano *et al.*, 2003; Dokka, Sella and Dixon, 2006), glacial isostatic adjustment (Gonzalez and Tornqvist, 2006), hydrocarbon extraction (Morton and Bernier, 2010), and artificial drainage (Dixon *et al.*, 2006)). Sediment diversions aim to restore

and nourish the wetlands by increasing elevation through new sediment input from the Mississippi River (Allison and Meselhe, 2010). Various small-scale dredge repurposing projects within the MD have been conducted over the past 30 years, showing promising results for the rehabilitation of uninhabited wetlands (Ford, Cahoon and Lynch, 1999; Baptist *et al.*, 2019), but sediment diversion plans are large-scale and perceived as cost effective over time (Wiegman *et al.*, 2018). Instead of active sediment redistribution, sediment diversions are a more "nature-based" solution to sediment starvation caused by levee and dam construction as they mimic fluvial crevasse splays and sediment delivery to receiving basins (Meade and Moody, 2010; Xu *et al.*, 2019).

In the GBM delta, embanked coastal lands are subsiding from lack of sediment input (Alam, 1996; Hoque and Alam, 1997; Auerbach *et al.*, 2015), and small scale sediment diversion operations, locally called Tidal River Management (TRM) have been implemented in Bangladesh to reduce waterlogging by increasing land elevation (Amir *et al.*, 2013; Khadim *et al.*, 2013; Hossain, Khan and Shum, 2015). TRM utilizes engineering to create a nature-based solution, similar to the planned diversion projects in the MD, but this practice is intended to raise inhabited lands, where millions of coastal people live. TRM consists of creating an artificial canal, called a link canal, to connect the embanked landscape to an adjacent tidal river channel (Amir *et al.*, 2013). During high tide, water enters the embankment through

the link canal, and suspended sediment is deposited during slack high water. With a higher sediment carrying capacity during ebb tide, the water flows out through the link canal, eroding sediment near the canal entrance and adjacent tidal channel (Amir et al., 2013). Thus, the benefits of TRM are two-fold – embanked landscapes gain elevation, and the external tidal channels increase in width and depth allowing for water to drain out of the embankment during low tide, reducing waterlogging (Mutahara et al., 2018). Previous studies postulate that TRM elevates the embankments by 1-3 m over a period of several years – alleviating flood risk in the near-future (Khadim et al., 2013; Gain et al., 2017; Tasich, Gilligan and Goodbred Jr., 2019; Adnan et al., 2020). Eventually, the link canals are closed, and the land can be inhabited and farmed once again.

While TRM results in raising the embanked landscape, it takes 3-5 years for the sediment to accumulate (Amir *et al.*, 2013; Khadim *et al.*, 2013; Tasich, Gilligan and Goodbred Jr., 2019). During this time, the landowners and inhabitants of the affected area are essentially unable to farm or work on the land, and they are commonly not compensated for this loss (Amir *et al.*, 2013). Additionally, TRM has only been implemented in small (~10 km²), low-lying areas called "beels", which were wetlands prior to human occupation; polders are much larger in scale, often exceeding 100 km². We propose that repurposing material that is currently being dredged from local tidal channels to maintain navigability and reduce water logging

can be used in conjunction with TRM or as a short-term solution to flooding. Specifically, we recommend repurposing this material to elevate houses and/or augment embankments. Repurposing the spoils has fewer social inconveniences because: (1) houses and embankments can be elevated immediately, and (2) the land can be used continuously. Certainly, TRM can be more sustainable for the future as it addresses the root of the problem of flooding by attenuating elevation deficits caused by preclusion of sediment, compaction, subsidence, and ESLR within the embanked lands. However, TRM does not provide immediate protection, and the entire process takes years, as mentioned earlier. In the meantime while mechanical dredging is an ongoing practice, dredge spoil repurposing has the potential to provide a relatively rapid and straightforward solution to flood risk, while still allowing for TRM in the future.

6. Conclusions

This study analyzed the elevations, channel infilling, and stratigraphy within and outside embankments in the southwest region of the GBM delta near the cities of Khulna, Dacope, and Rampal. Elevation studies revealed that embankments have starved the region of sediment, resulting in elevation differences of ~1-1.5m between the embanked land and adjacent, higher unembanked land, expanding earlier elevation studies from Auerbach et al. (2015). Stratigraphical analyses show the regional stratigraphy between both embanked and unembanked land is silt dominated. Factoring

in ESLR, the embanked lands are at considerable risk of inundation during flood events – the mMHW already exceeds the average embanked elevations at Khulna and Rampal (by 0.3 and 0.6 m depth, respectively), and the potential inundation depth will increase by >200% for Khulna and >67% for Rampal over the next 30 years. Using aerial imagery, channel width analyses revealed that channels proximal to the polders have all infilled over the past 30+ years – average channel widths near Khulna, Dacope, and Rampal have decreased by 39%, 87%, and 72%, respectively.

Channel infilling and width reduction pose a serious challenge to waterlogging, flood risk, and navigation, and the most common method to remedy the problems is mechanical dredging. However, the dredge spoils are deposited along the channels instead of being repurposed. This study proposes repurposing dredge spoils to elevate houses and embankments above the predicted mMHW for 2050, thus reducing the flood vulnerability of the embanked regions (as evidenced by elevation studies and ESLR). If all infilled tidal channels throughout the GBM delta are dredged to 10% of their original widths, approximately $46.2 \times 10^6 \, \mathrm{m}^3$ of sediment will be available for repurposing. This sediment could elevate $\sim 547,000$ houses or elevate $\sim 500 \, \mathrm{km}$ length of embankments. While TRM is a sustainable method of replenishing land elevations and maintaining navigability of surrounding channels, repurposing dredge spoils can protect the embanked lands from

- increasing storm surges and flooding in the near future, while allowing
- continued habitation and agricultural use of land.

729	References
730	Adnan, M. S. G. et al. (2020) 'The potential of Tidal River Management for
731	flood alleviation in South Western Bangladesh', Science of the Total
732	Environment, 731, p. 138747. doi: 10.1016/j.scitotenv.2020.138747.
733	Alam, M. (1996) 'Subsidence of the Ganges-Brahmaputra Delta of
734	Bangladesh and associated drainage, sedimentation and salinity problems',
735	Coastal Systems and Continental Margins, 2, pp. 169–192. Available at:
736	http://libezp.lib.lsu.edu/login?url=http://search.ebscohost.com/login.aspx?di
737	rect=true&db=geh&AN=1997-006545&site=ehost-live&scope=site.
738	Allison, M. A. and Kepple, E. (2001) 'Modern sediment supply to the lower
739	delta plain of the Ganges-Brahmaputra River in Bangladesh', Geo-Marine
740	Letters, 21(2), pp. 66-74. doi: 10.1007/s003670100069.
741	Allison, M. A. and Meselhe, E. A. (2010) 'The use of large water and
742	sediment diversions in the lower Mississippi River (Louisiana) for coastal
743	restoration', Journal of Hydrology, 387(3-4), pp. 346-360. doi:
744	10.1016/j.jhydrol.2010.04.001.
745	Amir, M. S. I. I. et al. (2013) 'Tidal River Sediment Management - A Case
746	Study in Southwestern Bangladesh', International Journal of Civil Science
747	and Engineering, 7(3), pp. 175–185.
748	Arifuzzaman, S. M. N. and Zaman, M. N. B. (2013) 'A Case Study on Cost
7/10	Effective Technique for Plinth Improvement of Rural Houses: Bangladesh

- 750 Perspective', 2(5), pp. 295–303.
- Arun, P. V. (2013) 'A comparative analysis of different DEM interpolation
- methods', Egyptian Journal of Remote Sensing and Space Science, 16(2),
- pp. 133–139. doi: 10.1016/j.ejrs.2013.09.001.
- Auerbach, L. W. et al. (2015) 'Flood risk of natural and embanked
- landscapes on the Ganges-Brahmaputra tidal delta plain', Nature Climate
- 756 *Change*, 5(2), pp. 153–157. doi: 10.1038/nclimate2472.
- Ayers, J. C. et al. (2017) 'Salinization and arsenic contamination of surface
- water in southwest Bangladesh', Geochemical Transactions, 18(1), pp. 1–23.
- 759 doi: 10.1186/s12932-017-0042-3.
- Bain, R. L., Hale, R. P. and Goodbred, S. L. (2019) 'Flow Reorganization in
- an Anthropogenically Modified Tidal Channel Network: An Example From the
- Southwestern Ganges-Brahmaputra-Meghna Delta', Journal of Geophysical
- 763 Research: Earth Surface, 124(8), pp. 2141–2159. doi:
- 764 10.1029/2018JF004996.
- Bangladesh Water Development Board (BWDB) (2013) 'Coastal embankment
- improvement project: Final report', I, pp. 1–2. Available at:
- 767 http://hdl.handle.net/2060/19920075773.
- Baptist, M. J. et al. (2019) 'Beneficial use of dredged sediment to enhance
- salt marsh development by applying a "Mud Motor", Ecological Engineering,
- 127(December 2018), pp. 312–323. doi: 10.1016/j.ecoleng.2018.11.019.

- Blum, M. D. et al. (2008) 'Ups and downs of the Mississippi delta', Geology,
- 36(9), pp. 675–678. doi: 10.1130/G24728A.1.
- Bomer, E. J. et al. (2020) 'Surface elevation and sedimentation dynamics in
- the Ganges-Brahmaputra tidal delta plain, Bangladesh: Evidence for
- mangrove adaptation to human-induced tidal amplification', Catena,
- 187(September 2019), p. 104312. doi: 10.1016/j.catena.2019.104312.
- Bomer, E. J., Wilson, C. A. and Datta, D. K. (2019) 'An integrated approach
- for constraining depositional zones in a tide-influenced river: insights from
- the Gorai River, Southwest Bangladesh', Water, 11(10), p. 2047.
- Brain, M. J. (2016) 'Past, Present and Future Perspectives of Sediment
- Compaction as a Driver of Relative Sea Level and Coastal Change', Current
- 782 Climate Change Reports, 2(3), pp. 75–85. doi: 10.1007/s40641-016-0038-
- 783 **6.**
- Brammer, H. (2014) 'Bangladesh's dynamic coastal regions and sea-level
- rise', Climate Risk Management, 1, pp. 51–62. doi:
- 786 10.1016/j.crm.2013.10.001.
- 787 Brandon, D. L. and Price, R. A. (2007) 'Summary of Available Guidance and
- 788 Best Practices for Determining Suitability of Dredged Material for Beneficial
- Uses Summary of Available Guidance and Best Practices for Determining
- Suitability of Dredged Material for Beneficial Uses', *Environmental*
- 791 *Laboratory*, (ERDC/EL TR-07-27), p. 104.

- Bricheno, L. M., Wolf, J. and Islam, S. (2016) 'Tidal intrusion within a mega
- delta: An unstructured grid modelling approach', Estuarine, Coastal and
- 794 Shelf Science, 182, pp. 12–26. doi: 10.1016/j.ecss.2016.09.014.
- Carrico, A. R. et al. (2020) 'Extreme weather and marriage among girls and
- women in Bangladesh', Global Environmental Change, 65(August), p.
- 797 102160. doi: 10.1016/j.gloenvcha.2020.102160.
- Chamberlain, E. L. et al. (2017) 'Luminescence dating of delta sediments:
- Novel approaches explored for the Ganges-Brahmaputra-Meghna Delta',
- 800 Quaternary Geochronology, 41(July 2018), pp. 97–111. doi:
- 801 10.1016/j.guageo.2017.06.006.
- Daliakopoulos, I. N. et al. (2016) 'The threat of soil salinity: A European
- scale review', *Science of the Total Environment*, 573, pp. 727–739. doi:
- 804 10.1016/j.scitotenv.2016.08.177.
- Daniels, W. L., Whittecar, G. R. and Carter, C. H. (2007) 'Conversion of
- 806 Potomac River dredge sediments to productive agricultural soils', *American*
- 807 Society of Mining and Reclamation 24th National Meetings of the American
- 808 Society of Mining and Reclamation 2007: 30 Years of SMCRA and Beyond,
- 2(November), pp. 597–613. doi: 10.21000/JASMR07010183.
- Dasgupta, S. et al. (2010) 'Vulnerability of Bangladesh to Cyclones in a
- 811 Changing Climate: Potential Damages and Adaptation Cost', World Bank
- 812 Policy Research Working Paper, (5280).

- Dasgupta, S. et al. (2015) 'River salinity and climate change: Evidence from
- coastal Bangladesh', World Scientific Reference on Asia and the World
- 815 *Economy*, (March), pp. 205–242. doi: 10.1142/9789814578622_0031.
- Davis, R. A. and Dalrymple, R. W. (2011) 'Principles of tidal sedimentology',
- 817 *Principles of Tidal Sedimentology*, pp. 1–621. doi: 10.1007/978-94-007-
- 818 0123-6.
- Dixon, T. H. et al. (2006) 'Subsidence and flooding in New Orleans', Nature,
- 820 441, pp. 587–588.
- Dokka, R. K., Sella, G. F. and Dixon, T. H. (2006) 'Tectonic control of
- subsidence and southward displacement of southeast Louisiana with respect
- to stable North America', *Geophysical Research Letters*, 33(23), pp. 1–5.
- 824 doi: 10.1029/2006GL027250.
- Duncan, J. M., Wright, S. G. and Brandon, T. L. (2014) 'Soil Strength and
- Slope Stability, 2nd Edition', John Wiley & Sons, p. 336.
- Dunn, F. E. et al. (2019) 'Projections of declining fluvial sediment delivery to
- major deltas worldwide in response to climate change and anthropogenic
- stress', Environmental Research Letters, 14(8). doi: 10.1088/1748-
- 830 9326/ab304e.
- Duo, L. and Hu, Z. (2018) 'Soil quality change after reclaiming subsidence
- land with Yellow River sediments', Sustainability (Switzerland), 10(11), pp.
- 833 1-13. doi: 10.3390/su10114310.

- EGIS (2000) Environmental Baseline of Gorai River Restoration Project, EGIS
- 835 *II*.
- Fan, X. et al. (2012) 'Soil salinity development in the yellow river delta in
- relation to groundwater dynamics', Land Degradation and Development,
- 838 23(2), pp. 175–189. doi: 10.1002/ldr.1071.
- Ford, M. A., Cahoon, D. R. and Lynch, J. C. (1999) 'Restoring marsh
- 840 elevation in a rapidly subsiding salt marsh by thin-layer deposition of
- dredged material', *Ecological Engineering*, 12(3–4), pp. 189–205. doi:
- 842 10.1016/S0925-8574(98)00061-5.
- Gagliano, S. M. et al. (2003) 'Neo-Tectonic Framework of Southeast
- Louisiana and Applications to Coastal Restoration', GCAGS/GCSSEPM
- 845 *Transactions*, 53, pp. 262–276. Available at: www.biodiversitybc.org.
- Gain, A. K. et al. (2017) 'Tidal river management in the south west Ganges-
- Brahmaputra delta in Bangladesh: Moving towards a transdisciplinary
- approach?', Environmental Science and Policy, 75(June), pp. 111–120. doi:
- 849 10.1016/j.envsci.2017.05.020.
- 850 Gonzalez, J. L. and Tornqvist, T. E. (2006) 'Coastal Louisiana in crisis:
- Subsidence or sea level rise?', *Eos*, 87(45), pp. 7–10. doi:
- 852 10.1029/2006EO450001.
- Hale, R. et al. (2019) 'Observations and scaling of tidal mass transport
- across the lower Ganges-Brahmaputra delta plain: Implications for delta

- management and sustainability', Earth Surface Dynamics, 7(1), pp. 231–
- 856 245. doi: 10.5194/esurf-7-231-2019.
- Haque, A. et al. (2019) 'A Cyclone Classifier Model for Real-time Cyclone
- Warning in Bangladesh', in 4th Global Summit of Research Institutes for
- 859 Disaster Risk Reduction. Kyoto, Japan.
- Hesselink, A. W., Weerts, H. J. T. and Berendsen, H. J. A. (2003) 'Alluvial
- architecture of the human-influenced river Rhine, The Netherlands',
- 862 Sedimentary Geology, 161(3-4), pp. 229-248. doi: 10.1016/S0037-
- 863 0738(03)00116-7.
- Holleman, R. C. and Stacey, M. T. (2014) 'Coupling of sea level rise, tidal
- amplification, and inundation', *Journal of Physical Oceanography*, 44(5), pp.
- 866 1439–1455. doi: 10.1175/JPO-D-13-0214.1.
- Holtz, R. D., Kovacs, W. D. and Sheahan, T. C. (1981) An Introduction to
- 868 Second Edition Geotechnical Engineering. Englewood Cliffs: Prentice-Hall.
- Hoque, M. and Alam, M. (1997) 'Subsidence in the lower deltaic areas of
- Bangladesh', *Marine Geodesy*, 20(1), pp. 105–120. doi:
- 871 10.1080/01490419709388098.
- Hossain, F., Khan, Z. H. and Shum, C. K. (2015) 'Tidal river management in
- Bangladesh', *Nature Climate Change*, 5(6), p. 492. doi:
- 874 10.1038/nclimate2618.

- 875 Khadim, F. K. et al. (2013) 'Integrated Water Resources Management
- 876 (IWRM) Impacts in South West Coastal Zone of Bangladesh and Fact-Finding
- on Tidal River Management (TRM)', Journal of Water Resource and
- 878 *Protection*, 05(10), pp. 953–961. doi: 10.4236/jwarp.2013.510098.
- 879 Khan, M. J. U. et al. (2020) 'Towards an efficient storm surge and inundation
- forecasting system over the Bengal delta: Chasing the super-cyclone
- 881 Amphan', Natural Hazards and Earth System Sciences, (October), pp. 1–29.
- 882 doi: 10.5194/nhess-2020-340.
- 883 Kulp, S. A. and Strauss, B. H. (2019) 'New elevation data triple estimates of
- global vulnerability to sea-level rise and coastal flooding', Nature
- 885 *communications*, 10(1), pp. 1–12.
- 886 Majumdar, S. C. (1941) 'Rivers of the Bengal Delta'. Bengal Government
- 887 Press, p. 68.
- 888 Mao, W. et al. (2016) 'Yellow River Sediment as a Soil Amendment for
- Amelioration of Saline Land in the Yellow River Delta', Land Degradation and
- 890 *Development*, 27(6), pp. 1595–1602. doi: 10.1002/ldr.2323.
- 891 Mao, W. et al. (2018) 'Applying dredged sediment improves soil salinity
- environment and winter wheat production', Communications in Soil Science
- 893 *and Plant Analysis*, 49(14), pp. 1787–1794. doi:
- 894 10.1080/00103624.2018.1474915.
- Meade, R. H. and Moody, J. A. (2010) 'Causes for the decline of suspended-

- sediment discharge in the Mississippi River system, 1940-2007', *Hydrological*
- 897 *Processes*, 24, pp. 35–49. doi: 10.1002/hyp.
- Meckel, T. A., Ten Brink, U. S. and Williams, S. J. (2007) 'Sediment
- compaction rates and subsidence in deltaic plains: Numerical constraints and
- stratigraphic influences', Basin Research, 19(1), pp. 19–31. doi:
- 901 10.1111/j.1365-2117.2006.00310.x.
- 902 Mirza, M. M. Q. (1998) 'Diversion of the Ganges water at Farakka and its
- effects on salinity in Bangladesh', *Environmental Management*, 22(5), pp.
- 904 711-722. doi: 10.1007/s002679900141.
- Morton, R. A. and Bernier, J. C. (2010) 'Recent subsidence-rate reductions in
- 906 the Mississippi delta and their geological implications', Journal of Coastal
- 907 Research, 26(3), pp. 555–561. doi: 10.2112/JCOASTRES-D-09-00014R1.1.
- 908 Mukerjee, R. (1938) 'The Changing Face of Bengal: A Study in Riverine
- 909 Economy', Calcutta University Readership Lectures, p. 289.
- 910 Mutahara, M. et al. (2018) 'Social learning for adaptive delta management:
- Tidal River Management in the Bangladesh Delta', International Journal of
- 912 Water Resources Development, 34(6), pp. 923–943. doi:
- 913 10.1080/07900627.2017.1326880.
- 914 Pethick, J. and Orford, J. D. (2013) 'Rapid rise in effective sea-level in
- southwest Bangladesh: Its causes and contemporary rates', *Global and*
- 916 Planetary Change, 111(October), pp. 237–245. doi:

- 917 10.1016/j.gloplacha.2013.09.019.
- Rahman, M. M. et al. (2013) 'Assessing The Causes of Deterioration of the
- 919 Mongla-Ghashiakhali Navigation Route for Restoration of Navigability', in
- 920 International Conference on Climate Change Impact and Adaptation (I3CIA-
- 921 *2013*). Gazipur, Bangladesh, pp. 1–9.
- Rahman, M. M. et al. (eds) (2019) Integrated Assessment for the
- 923 Bangladesh Delta Plan 2100: Analysis of selected interventions. BUET-
- 924 Southampton University-GED, Planning Commission, People's Republic of
- 925 Bangladesh.
- 926 Shampa, M. and Pramanik, I. M. (2012) 'Tidal River Management (TRM) for
- 927 Selected Coastal Area of Bangladesh to Mitigate Drainage Congestion',
- International Journal of Scientific and Technology Research, 1(5), pp. 1–6.
- 929 Available at: http://www.ijstr.org/final-print/june2012/Tidal-River-
- 930 Management-(Trm)-of-Selected-Coastal-Area-of-Bangladesh-For-Mitigation-
- 931 of-Drainage-Congestion.pdf.
- Sheehan, C. and Harrington, J. (2012) 'Management of dredge material in
- the Republic of Ireland A review.', *Waste Management*, 32, pp. 1031–1044.
- 934 Shepard, F. P. (1954) 'Nomenclature Based on Sand-Silt-Clay Ratios',
- Journal of Sedimentary Petrology, 24(3), pp. 151–158. doi:
- 936 10.1306/D4269774-2B26-11D7-8648000102C 1865D.
- 937 Smajgl, A. et al. (2015) 'Responding to rising sea levels in the Mekong

- 938 Delta', Nature Climate Change, 5(2), pp. 167–174. doi:
- 939 10.1038/nclimate2469.
- 940 Sultana, P., Uddin, M. I. and Analysis, M. (2017) 'Dredging and Land
- 941 Reclamation in Bangladesh Perspective: A State-of-the- Art Overview
- Dredging and Land Reclamation in Bangladesh Perspective: A State-of-the-
- 943 Art Overview', (February), pp. 0–4.
- 944 Syvitski, James P. M. et al. (2009) 'Sinking Deltas', Nature Geoscience,
- 945 2(10), pp. 681–686.
- 946 Syvitski, James P.M. et al. (2009) 'Sinking deltas due to human activities',
- 947 *Nature Geoscience*, 2(10), pp. 681–686. doi: 10.1038/ngeo629.
- Tasich, C. M., Gilligan, J. M. and Goodbred Jr., S. L. (2019) 'Coupled
- 949 Modeling of Landscape Evolution and Human Adaptation in the Ganges-
- 950 Brahmaputra Delta', in AGU Fall Meeting.
- The Daily Star (2020) 'Mega plan taken up to dredge 178 rivers', The Daily
- 952 *Star*, 10 February. Available at:
- 953 https://www.thedailystar.net/backpage/news/178-rivers-be-dredged-
- 954 1865644.
- Törnqvist, T. E. et al. (2008) 'Mississippi Delta subsidence primarily caused
- by compaction of Holocene strata', *Nature Geoscience*, 1(3), pp. 173–176.
- 957 doi: 10.1038/ngeo129.

- Wang, J. et al. (2012) 'Evaluation of the combined risk of sea level rise, land
- subsidence, and storm surges on the coastal areas of Shanghai, China',
- 960 Climatic Change, 115(3-4), pp. 537-558. doi: 10.1007/s10584-012-0468-7.
- Whitehead, P. G. et al. (2015) 'Impacts of climate change and socio-
- economic scenarios on flow and water quality of the Ganges, Brahmaputra
- and Meghna (GBM) river systems: low flow and flood statistics',
- 964 Environmental Science: Processes & Impacts, 17(6), pp. 1057–1069. doi:
- 965 10.17226/21507.
- Wiegman, A. R. H. et al. (2018) 'Modeling impacts of sea-level rise, oil price,
- and management strategy on the costs of sustaining Mississippi delta
- marshes with hydraulic dredging', Science of the Total Environment, 618,
- pp. 1547–1559. doi: 10.1016/j.scitotenv.2017.09.314.
- 970 Wilcox, W. (1930) 'Ancient System of Irrigation in Bengal'. University of
- 971 Calcutta, p. 90.
- 972 Wilson, C. et al. (2017) 'Widespread infilling of tidal channels and navigable
- waterways in the human-modified tidal deltaplain of southwest Bangladesh',
- 974 *Elementa*, 5. doi: 10.1525/elementa.263.
- 975 Winterwerp, J. C. and Giardino, A. (2012) 'Assessment of increasing
- 976 freshwater input on salinity and sedimentation in the Gorai river system',
- 977 (January), p. 63. doi: 10.13140/2.1.1504.1286.
- Yu, K. et al. (2019) 'A review of sediment diversion in the Mississippi River

979	Deltaic Plain', Estuarine, Coastal and Shelf Science, 225(May), p. 106241.
980	doi: 10.1016/j.ecss.2019.05.023.

Figure Captions

984

985

986

987

988

989

990

991

992

993

994

995

996

997

998

999

983

Figure 1. Study region in the southwest GBM delta located near Khulna, Dacope, and Rampal with embankments outlined in black. Elevation is created from CoastalDEM (© Climate Central), a 3 arcsecond (90 m) horizontal resolution corrected from SRTM (2000) data, with elevation relative to EGM 96. All elevations equal to or less than 0 meters are shaded blue. The fluvial-tidal delta plain and tidal delta plain are geographically divided by the Baleswari River; west of the Baleswari River, there is minimal fluvial input. Inset B is a closer view of three representative tidal channels off the Pussur River, near their respective cities. Similar to many channels in the SW GBM delta, these once-active tidal channels are silting in, impeding water navigation (see Fig. 3). Periodically, these channels are dredged to maintain navigability (see Figs. 2 & 4). The additional white boxes on the right are the coring locations shown in Figure 3. The dashed white box indicates the location of cores previously collected by Wilson et al. (2017) and Chamberlain et al. (2017).

1000

1001

1002

Figure 2. (A) Active dredging operations near Rampal in October 2019 and (B) Khulna 3 years post-dredging in October 2019. Dredge spoils are

deposited on either side of the channels, forming an artificial levee outside of existing polders (outlined in white). See Figure 1 for site locations.

Figure 3. Core locations from Khulna and Rampal sites (see Figure 1 for site locations). A total of 12 cores were taken – 3 outside the embankments (blue) and 3 inside the embankments (pink) for both sites.

Figure 4. Cross-sections with elevation and lithology of cores from the unembanked ("out", left) and embanked ("in", right) Khulna sites. The unembanked cores were taken across a point bar and cutbank along the Rupsa-Pussur River ~60km upstream of the mouth near Khulna. The channel has been silting in for decades, and dredging operations were ongoing from 2015-2020; the cross-section also displays where dredge spoils have been emplaced post-2017. Average elevation inside the embankment is much lower than outside the embankment. The stratigraphy is similar at depth with sandy silts being overlain by silt. However, the unembanked cores have more sandy silt packages near the surface, which is indicative of hydrologic connectivity with the tides. The elevations for the embanked and unembanked Rampal sites also offset from each other by ~1 m, and the stratigraphy closely resembles the Khulna sites – sandy silts at depth with finer silts near the surface.

Figure 5. (A) Astronomical tide predictions for Mongla during a spring-neap cycle in October 2019 (~15 km southwest of Rampal sites on the Pussur River; data provided by Bangladesh Inland Water Transport Authority [BIWTA]), along with measured water level obtained using a HOBO® pressure sensor on October 26 at Rampal sites outside of the embankment (locations in Fig. 1). The dashed pink line denotes the average embanked elevation at Rampal while the light blue line represents the averaged unembanked elevations (see Table 1). As evidenced by the graph, the water level at the nearest tide gauge station exceeds the Rampal embankment elevations during seasonal spring high tides, noted by the monthly mean high water for 2019 [mMHW(2019)]. (B) Number of days when the measured maximum water level at Mongla exceeded the average embanked Rampal elevation (2.91 m relative to EGM 96).

Figure 6. Representative vibracore stratigraphy from the non-embanked Rampal site (Rampal_out_1). A) Entire core from 0 to 363 cm. B) Picture of 0-33 cm in the core, where tidal rhythmites, cross-bedding, and lenticular bedding were observed. C) Tidal rhythmites at 180-190 cm. D) Mottled bedding at 346-378 cm. E) Core lithologic column displaying median grain size (D50).

Figure 7. (A) Changes in water volume (m³) of three representative tidal channels in the southwest GBM delta from 1984 to 2020. A decrease in water volume results from silting in measured from a reduction in the average channel width. All three channels have significantly silted in since 1984. (B) Google Earth images of the Khulna site for years 2000, 2003, 2017, and 2019. Channel width reduction from siltation can be observed in the upper reaches (>10 km upstream of mouth; >transect 50). Dredging operations were ongoing from 2015-2020.

Figure 8. Box and whisker plot of the measured elevation points for the embanked (pink) and unembanked (blue) sites near Khulna (left) and Rampal (right). The upper outliers for both embanked sites are the elevations along the embankments themselves. The lower outliers for the embanked sites near Khulna are points measured in an aquaculture pond. The dark gray boxes mark the boundaries of the monthly Mean High Water (mMHW) and monthly Mean Low Water (mMLW) in 2019 for the Khulna and Rampal sites, while the lighter gray boxes mark the boundaries of the mMHW and mMLW predicted by 2050 for both sites. Note that while the mMHW is higher at Rampal, Khulna experiences greater ESLR (most noticeable in the mMLW) as indicated by Pethick and Orford, 2013.

1067

1068

1069

Figure 9. Two methods of repurposing dredge spoils. (A) Elevating houses above Mean High Water (MHW) by constructing housing plinths and (B) elevating existing polders above MHW and storm surge levels (modified from Dasgupta *et al.*, 2010).

Tables

1072 **Table 1**

			Height
Locations	Latitude	Longitude	(relative to EGM 96, m)
Khulna_out_1	22.800567°	89.637325°	5.45
Khulna_out_2	22.799805°	89.635692°	3.08
Khulna_out_3	22.799995°	89.634790°	4.44
Khulna_out_avg†			4.54 ± 0.06
Khulna_in_1	22.772268°	89.652463°	1.88
Khulna_in_2	22.769355°	89.652346°	2.08
Khulna_in_3	22.755045°	89.652881°	3.00
Khulna_in_avg†			2.86 ± 0.04
Rampal_out_1	22.605659°	89.652447°	2.96
Rampal_out_2	22.604081°	89.651358°	2.91
Rampal_out_3	22.594744°	89.654705°	2.55
Rampal_out_avg†			3.98 ± 0.09
Rampal_in_1	22.593812°	89.658463°	2.42
Rampal_in_2	22.594336°	89.657483°	2.83
Rampal_in_3	22.593569°	89.656903°	2.86
Rampal_in_avg†			2.91 ± 0.03

†number of elevation points for each average:

Khulna_out_avg = 472 Khulna_in_avg = 354 Rampal_out_avg = 109 Rampal_in_avg = 258

Table 1: The core locations with respective heights measured with the Leica RTK GNSS system. Also listed are the average elevations for all 4 sites. Note that elevations decrease with proximity to the coast, and elevation inside the embankments is $\sim 1-1.7$ m lower than outside the embankments (see also Fig. 8).

1078

1073

1074

1075

1076

1077

Table 2

Water Volumes and Subsequent Dredge Spoil Volumes for Study Sites

101 0144 01100						
	Water Volume in 1984 (m³)	Pre-Dredging Water Volume (m³)*	Post- Dredging Water Volume (m³)*	Total Amount of Sediment Removed (m³)†		
Khulna	6,861,083	421,218	1,159,788	738,570		
Dacope	16,183,502	384,326	800,248	415,922		
Rampal	7,618,765	241,796	781,113	539,317		

†Indicates volumes that are only representative of dredged areas.

For Khulna – transects 50-100; Dacope – all transects; Rampal – transects 1-70

The initial water volume is calculated for all transects for all three locations.

Table 2. The total water volumes of the three study tidal channels in 1984 (column 2). The proceeding volumes (columns 3-5) only consider transects that were dredged. For Dacope, all transects were dredged, but only transects 50-100 and 1-70 were dredged for Khulna and Rampal, respectively. While Dacope had the greatest infilling, it had the least amount of sediment dredged.

1094

1095

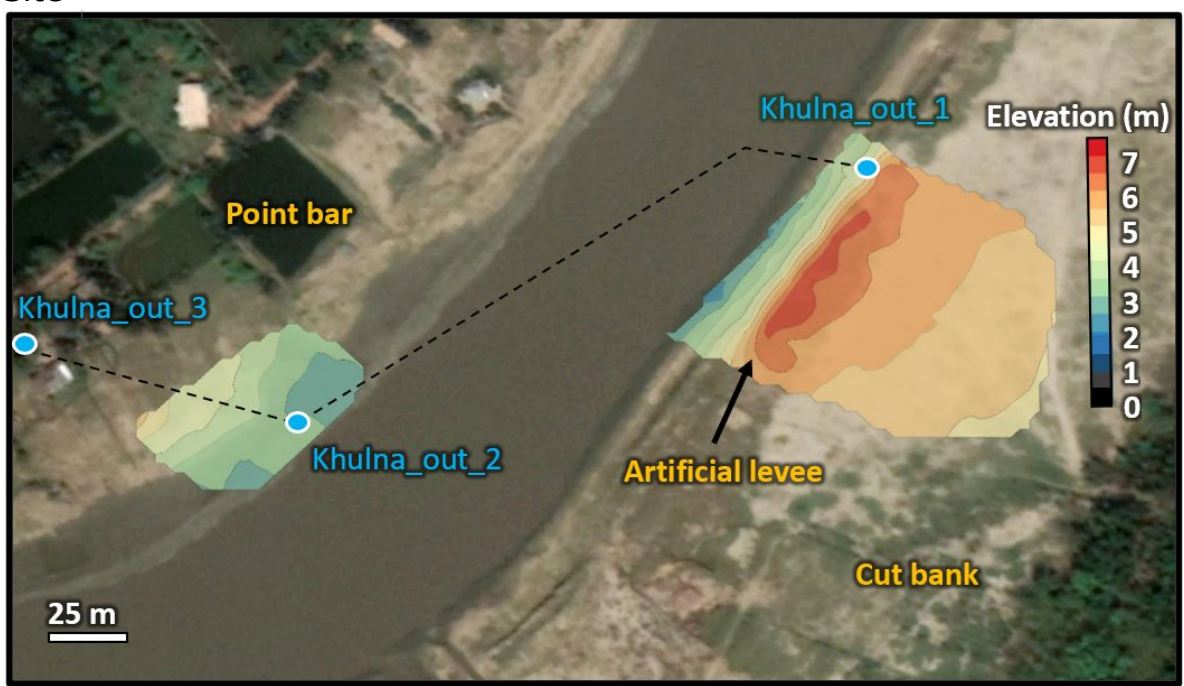
SUPPLEMENTAL MATERIAL

Supplemental Contains the Following Sections:

- 1) Elevation Survey
- 2) Tide Datums and Conversion of PWD to EGM 96
- 3) Coring and Sedimentological Data
- 4) Dredge Spoil Consolidation and Compaction
- 5) Channel Infilling Analyses and Geometric Calculations

1) Elevation Survey

Example of elevation survey measured with Leica GNSS at Khulna_out Site



Supplemental Figure S1: Google Earth Imagery from January 2019 of the Khulna non-embanked site with elevation contours (from ~420 GPS points) overlain. Note the cutbank has a much higher average elevation than the point bar, however, the highest points along the cutbank are from the placement of dredge spoil along the length of the river, forming an artificial levee.

2) Tide Datums and Conversion of PWD to EGM 96

Water level data for Mongla is available from multiple sources, but the tide datums vary. Bangladesh Inland Water Transport Authority (BIWTA) uses the Public Works Datum (PWD), which was assumed to be the MSL at Calculatta over 100 years ago. The Bangladesh Water Development Board (BWDB) uses the Chart Datum (CD), which is based on "Indian Spring Low Water" and uses an extended harmonic analysis as detailed in Mondal (2001). BIWTA then converts their CD data to MSL by subtracting 1.54 m. Auerbach et al. (2015) recorded their water levels with respect to the Earth Gravitational Model 1996 (EGM 96), which is a geodetic datum.

There are disagreements in the literature on the relationship between PWD (Public Works Datum) and MSL with respect to Bangladesh. Multiple sources state that PWD = MSL + 0.46 m (Choudhury, Paul and Paul, 2004; Hussain and Hoque, 2020), while others state PWD = MSL – 0.46 m (Jakobsen *et al.*, 2006; Amin *et al.*, 2015; Islam, Hofstra and Sokolova, 2018). Based on tide and elevation data recorded here, it appears that PWD is in fact below MSL. However, the conversion of 0.46 m was established over 50 years ago, and is based on the MSL at the Karnaphuli River in Chittagong (Mondal and Bangladesh Inland Water Transport Authority, 2001). The mean tidal range at Chittagong is ~50% greater than at the Sundarbans on the southwest coast (EGIS, 2000), meaning the relationship

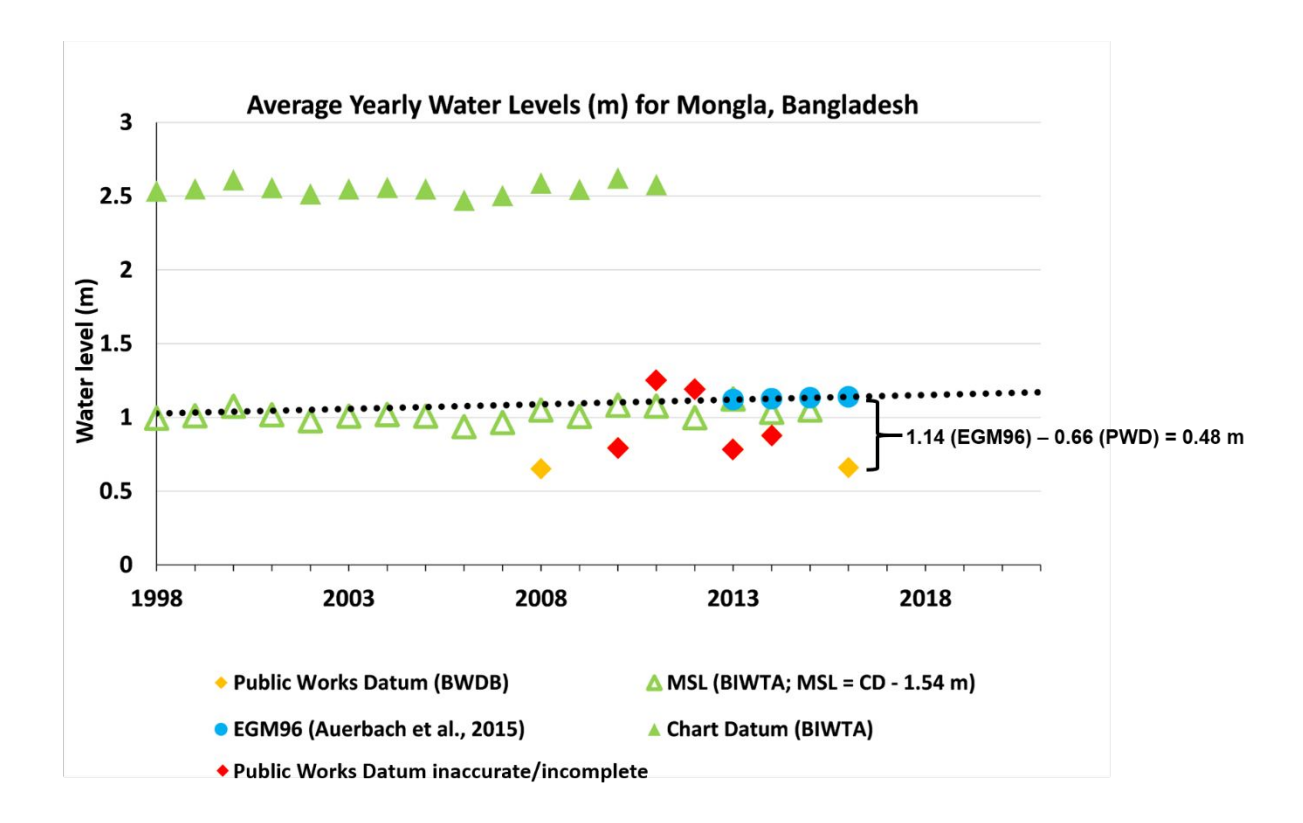
of PWD to MSL for Chittagong is not applicable to the study area.

Additionally, there is no established conversion between CD and PWD.

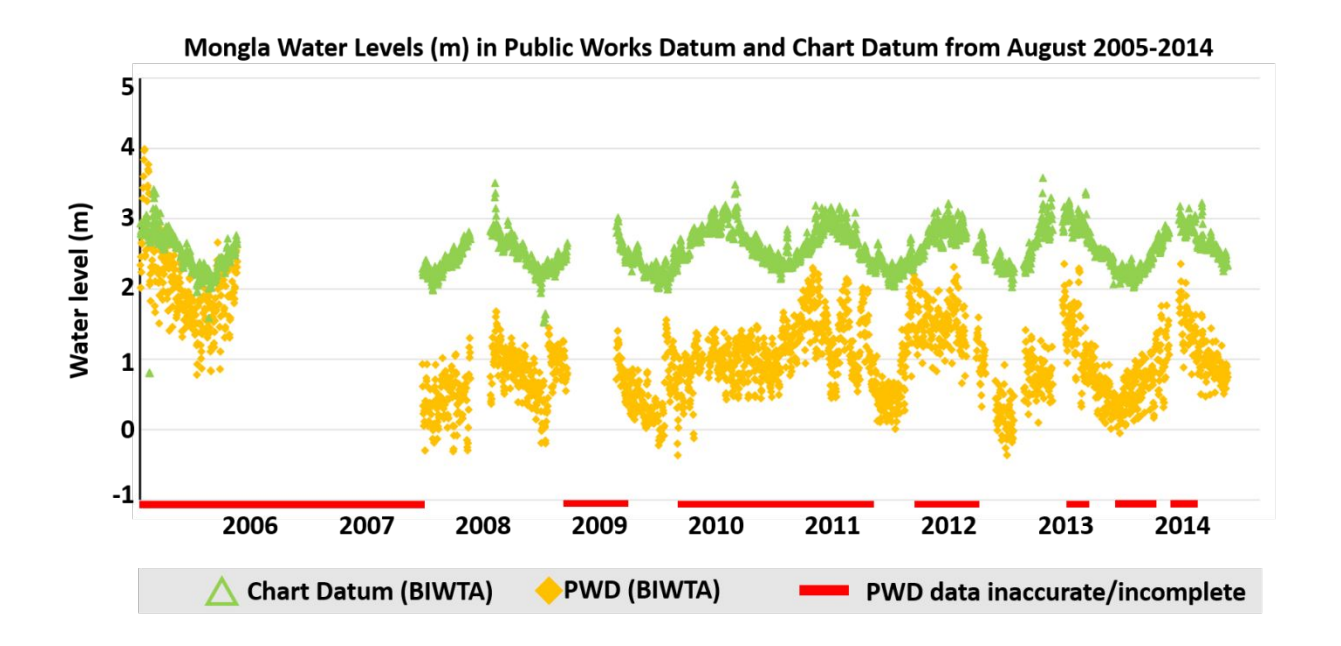
Ultimately, we used the MSL calculated by Auerbach et al. (2015), 1.12 m EGM 96, which was measured near Mongla in 2012-2013 (Fig. S2). Auerbach et al. (2015) calculated the MSL (1.12 m EGM 96) based on pressure gauge data collected at 10-minute intervals, with the instrument height being surveyed with a GPS unit to tie the data to the EGM 96 geodetic datum. This value for mean sea level closely agrees with BIWTA's MSL (which was converted from CD by subtracting 1.54 m) for the same time period, which is 1.11 m. While BIWTA's calculated MSL closely agrees with Auerbach's (2015) EGM 96 MSL, Pethick and Orford (2013) base their sea-level rise calculations on PWD; thus, we need to compare EGM 96 with PWD.

Tide gauge information for Mongla (in m PWD) was available from August 2005-December 2014 and January 2015 – March 2016. The PWD values for the time that was concurrent with Auerbach et al. (2015) were not used due to inaccuracies (Fig. S3), but the January 2015 – March 2016 data did not have any discernible errors; therefore, the 2015-2016 water levels (mPWD) were used for comparison. The MSL, or average of all the values, for this data is 0.66 m PWD (Fig. S2). Using the rate of MSL change for Mongla (6.25 mm a^{-1}) from Pethick and Orford (2013), we calculated that the MSL for Mongla in 2016 = 1.12 + (3 x 0.00625 m) = 1.14 m in EGM 96 (Fig. S2). The difference between the two MSL values for Mongla in 2016 is 0.48 m

(1.14 m (EGM 96) – 0.66 m (PWD)). Therefore, we conclude that EGM 96 \approx PWD + 0.48 m for the southwest region of Bangladesh.



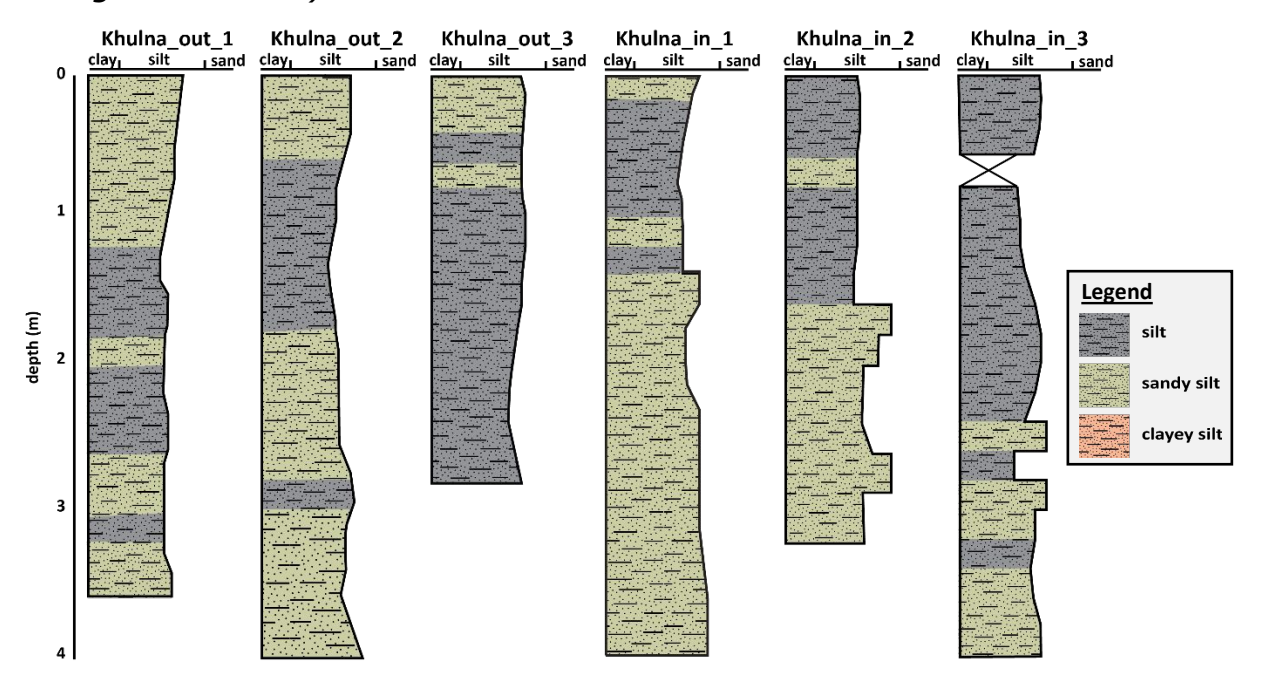
Supplemental Figure S2: Water Level Data for Mongla, Bangladesh, from 1998-2016 from various sources. The black trendline represents Pethick and Orford's (2013) estimate for relative mean sea level for Mongla (based on water levels from 1998-2010), which is 0.00625 m year⁻¹. While PWD water levels were measured during 2012-2013, the data has inaccuracies (detailed further in Fig. S3).



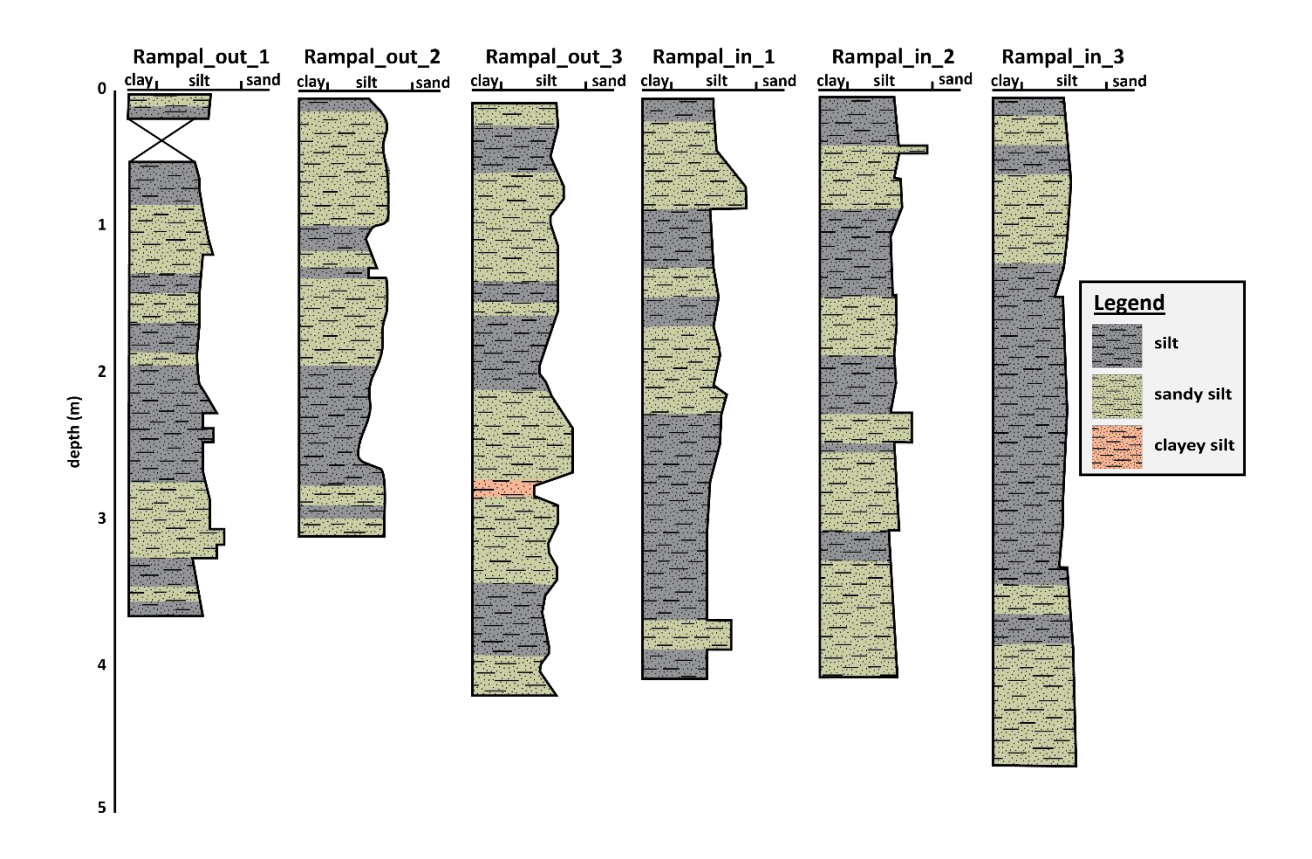
Supplemental Figure S3: Water level data for Mongla in two different tide datums – PWD and CD. The PWD is from BWDB, and the CD is from BIWTA. The Chart Datum values are typical of what's seen in the GBM Delta, with monsoon and dry season fluctuations as well as spring and neap tide fluctuations. The red lines indicate time ranges when the CD data is standard, but the PWD data is inconsistent. Even though PWD data was available during the time (2012-2013) of pressure gauge data from Auerbach et al. (2015), the PWD data was not used due to its inaccuracies during that time.

3) Coring and Sedimentological Data

Core lithology and geotechnical measurements (bulk density, grain size, organic content) for all core locations



Supplemental Figure S4: Core stratigraphy and grain size distribution at the embanked and non-embanked sites at Khulna (Khulna_in_1,2,3 and Khulna_out_1,2,3, respectively). Core locations shown in Fig 3 in main text. All cores were silt dominated with all cores having sandy silt beds throughout, with overall average grain size ranging from medium to coarse silt, median grain size $12.8-66.53 \, \mu m$ (6.29 to $3.9 \, \Phi$) for each core.



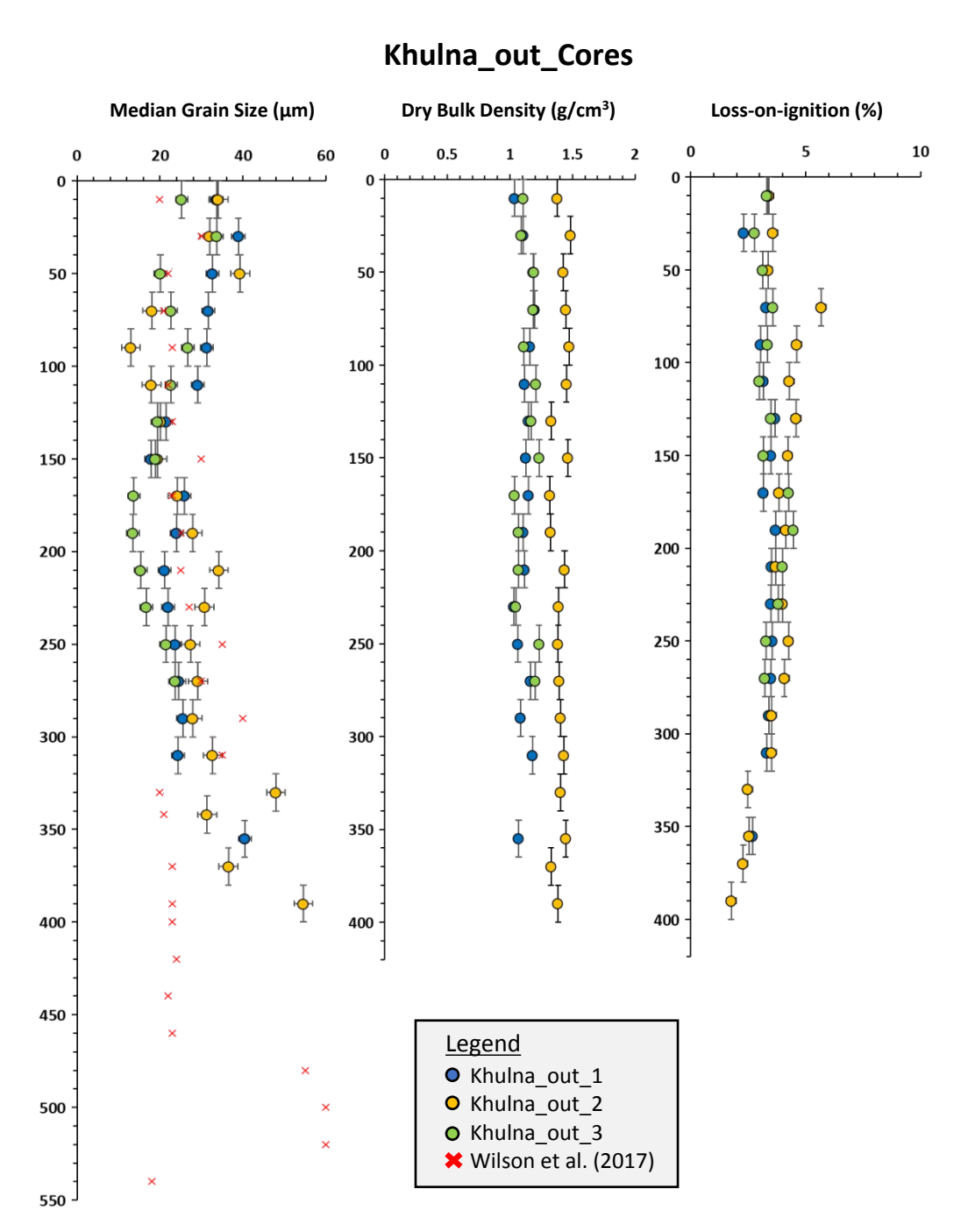
Supplemental Figure S5: Core stratigraphy and grain size distribution at the embanked and non-embanked sites at Rampal (Rampal_in_1,2,3, and Rampal_out_1,2,3, respectively). Core locations shown in Fig 3 in main text. All cores were silt dominated with all cores having sandy silt beds throughout, and one clayey silt bed for Rampal_out_3 from 262-273 cm. The overall average grain size ranged from medium to coarse silt, with median grain size $19.46-81.05~\mu m$ ($5.68~to~3.62~\Phi$) for each core.

For the cores outside the embankment near Khulna (Khulna_out_cores), there is minimal change in bulk density with depth (ranging from 1.0-1.5 g/cm³; averaging 1.2 ± 0.2 g/cm³), the organic matter determined from loss-on-ignition also varies minimally, ranging from 1.8-5.7% and averaging $\sim 3.5 \pm 0.7$ % for each core. All three cores were silt dominated, with no clear fining-upward or coarsening-upward sequences. These cores displayed similar grain size to that found by Wilson et al. (2017)

in an infilling channel near Dacope (Fig. 1; Supplemental figures S6-S9), and there similarly appears to be no discernible pattern between depth and grain size . The presence of tidalites and other small bedding structures such as flaser and lenticular bedding were visible in the cut cores (Fig. 6), but are evidenced by small fluctuations in grain size. The embanked Khulna cores (Khulna_in_), like the Khulna_out_cores, do not exhibit any relationship between bulk density and depth (ranging from 1.0-1.5 g/cm³, averaging 1.3 ± 0.1 g/cm³) but grain size does appear to slightly fine upwards. The organic content of the embanked cores has a slightly larger range of 2.2-7.4 %, averaging 4.3 ± 1.1 %. The depths with the highest organic matter percentages were from ~ 50 -100 cm.

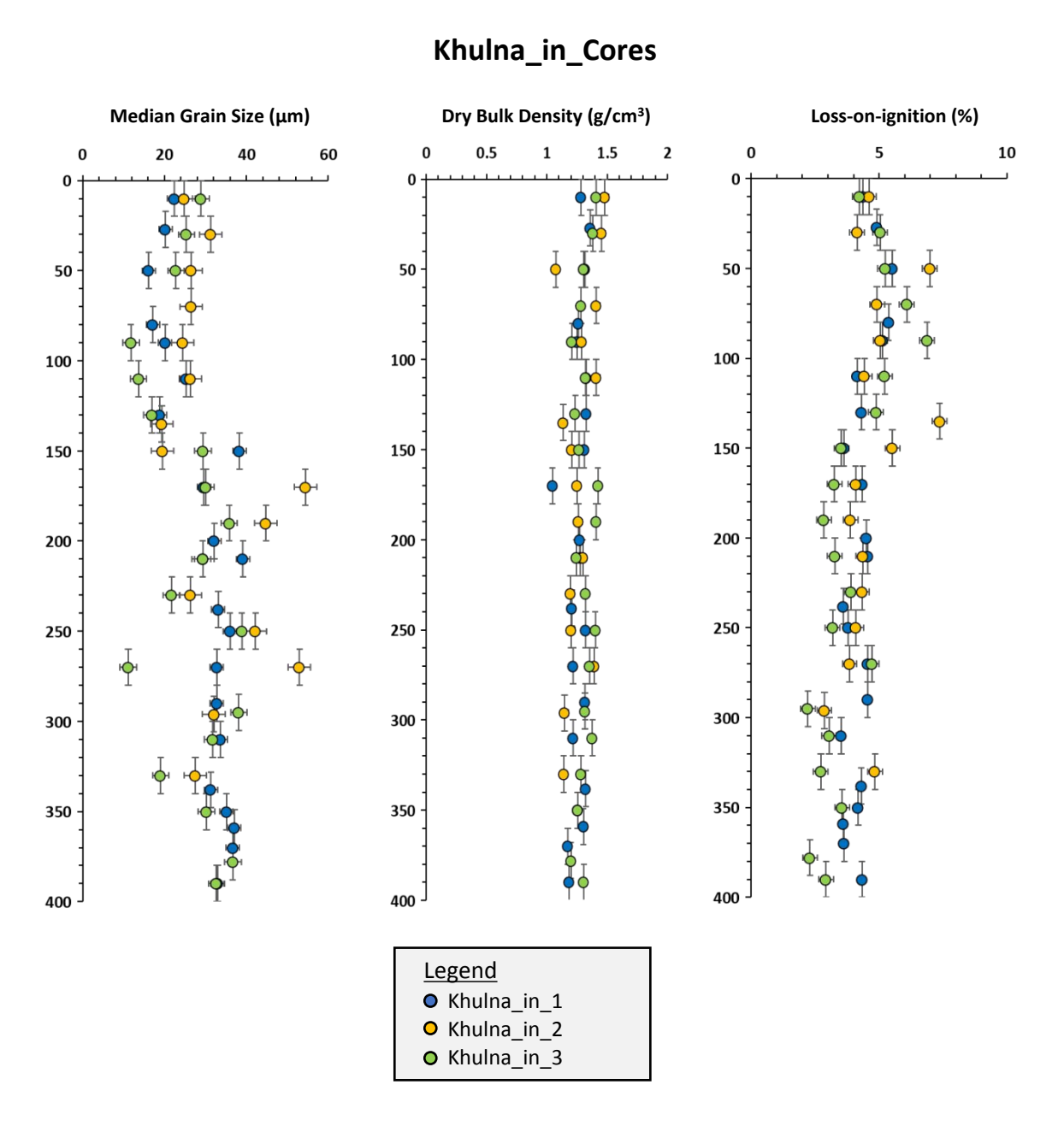
For the cores outside the embankment near Rampal (Rampal_out_), the bulk densities ranged from 1.1-1.8 g/cm³, averaging 1.4 ± 0.2 g/cm³. Rampal_out_1,2 displayed a slight increase in bulk density with relation to depth, but Rampal_out_3 displayed no such relationship. The percent organic matter for all Rampal_out_cores averaged $4.2 \pm 1.3\%$, ranging from 1.6 - 12.4%. The embanked Rampal cores (Rampal_in_) all show a slight increase in bulk density with increasing depth, and the values range from 1.1 - 1.8 g/cm³, averaging 1.4 ± 0.2 g/cm³. The median grain size for Rampal_in_1,2,3 shows no discernible pattern. The percent organic matter for Rampal_in_2,3 decreases with depth, while there is no apparent relationship between percent organic matter and depth for Rampal_in_1.

The percent organic matter for all 3 cores ranges from 2.7 - 7.6 %, averaging $4.4 \pm 1.0\%$.

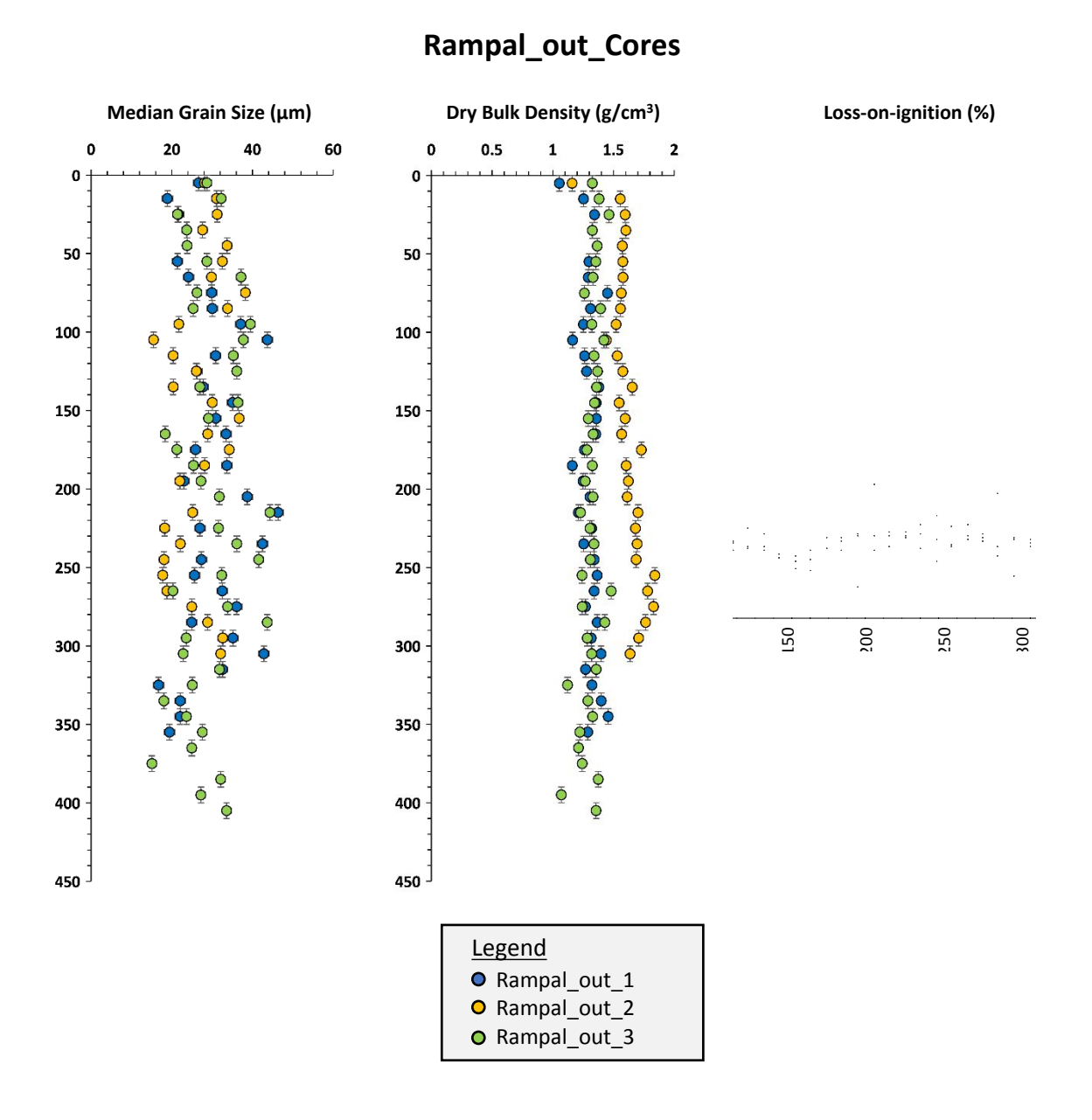


Supplemental Figure S6: Median grain size (μ m), dry bulk density (g/cm³) and loss-onignition % for all Khulna_out_ cores. The median grain size for the KHLC core in Wilson et al. (2017) is also graphed for comparison. The depth for the Wilson core extends to 540cm. Horizontal error bars for dry bulk density and loss-on-ignition (LOI) are standard error for all samples within a core, while the vertical error bars are fixed at 10cm as the samples

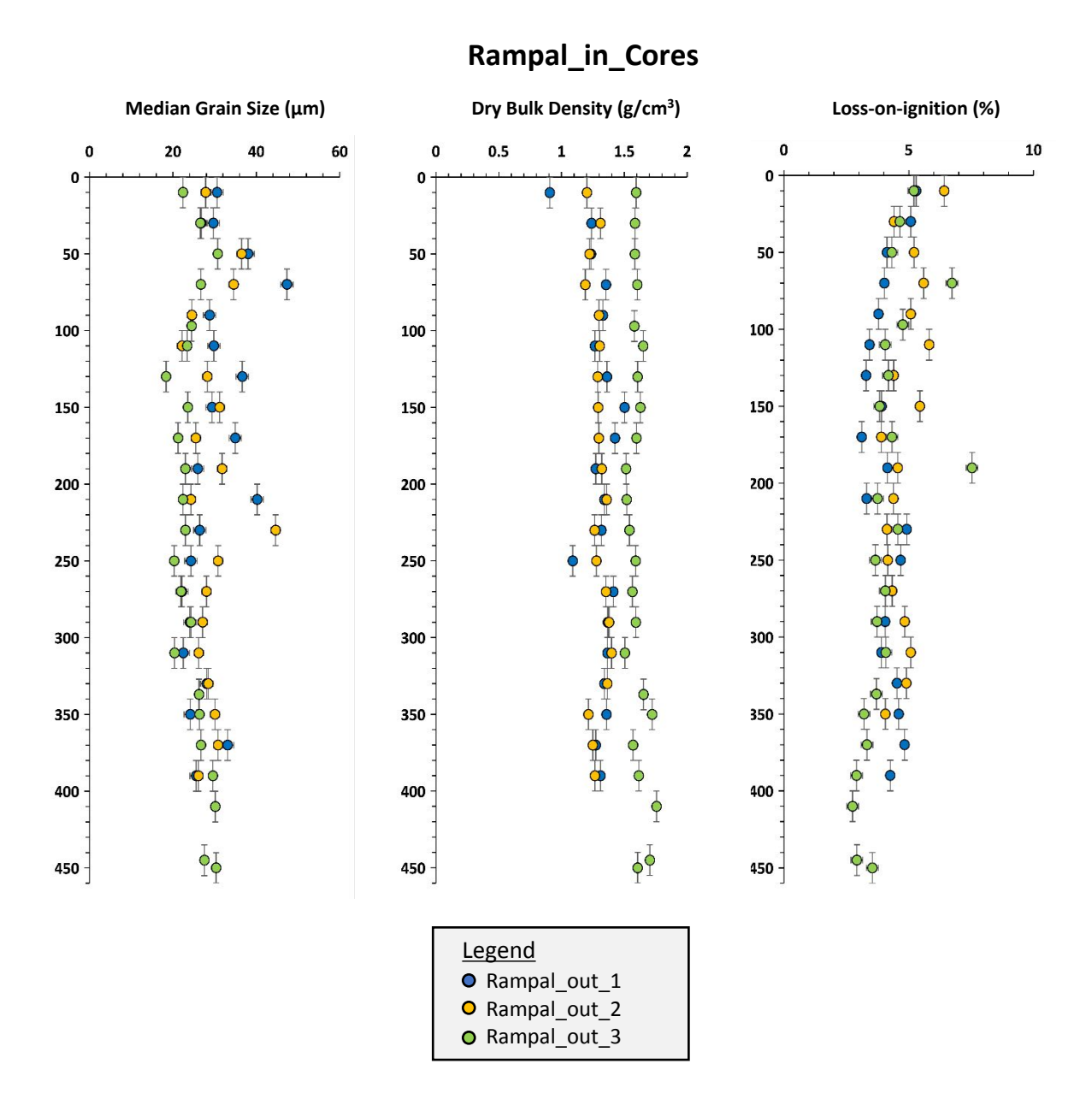
were collected in 20 cm intervals. Median grain size is predominantly silt and fines upwards for Khulna_out_1 and Khulna_out_2. LOI % values were all relatively low (<6%), indicating low organic matter, and the bulk densities ranged from 1.0 to 1.5 g/cm³.



Supplemental Figure S7: Median grain size (μ m), dry bulk density (g/cm^3) and loss-onignition % for all Khulna_in_ cores. Horizontal error bars for dry bulk density and loss-onignition are standard error for all samples within a core, while the vertical error bars are fixed at 10cm as the samples were collected in 20 cm intervals. Median grain size is predominantly silt and generally fines upwards for all 3 cores. LOI % values were all relatively low (<7.5%), indicating low organic matter, and the bulk densities ranged from 1.0 to 1.5 g/cm^3 .



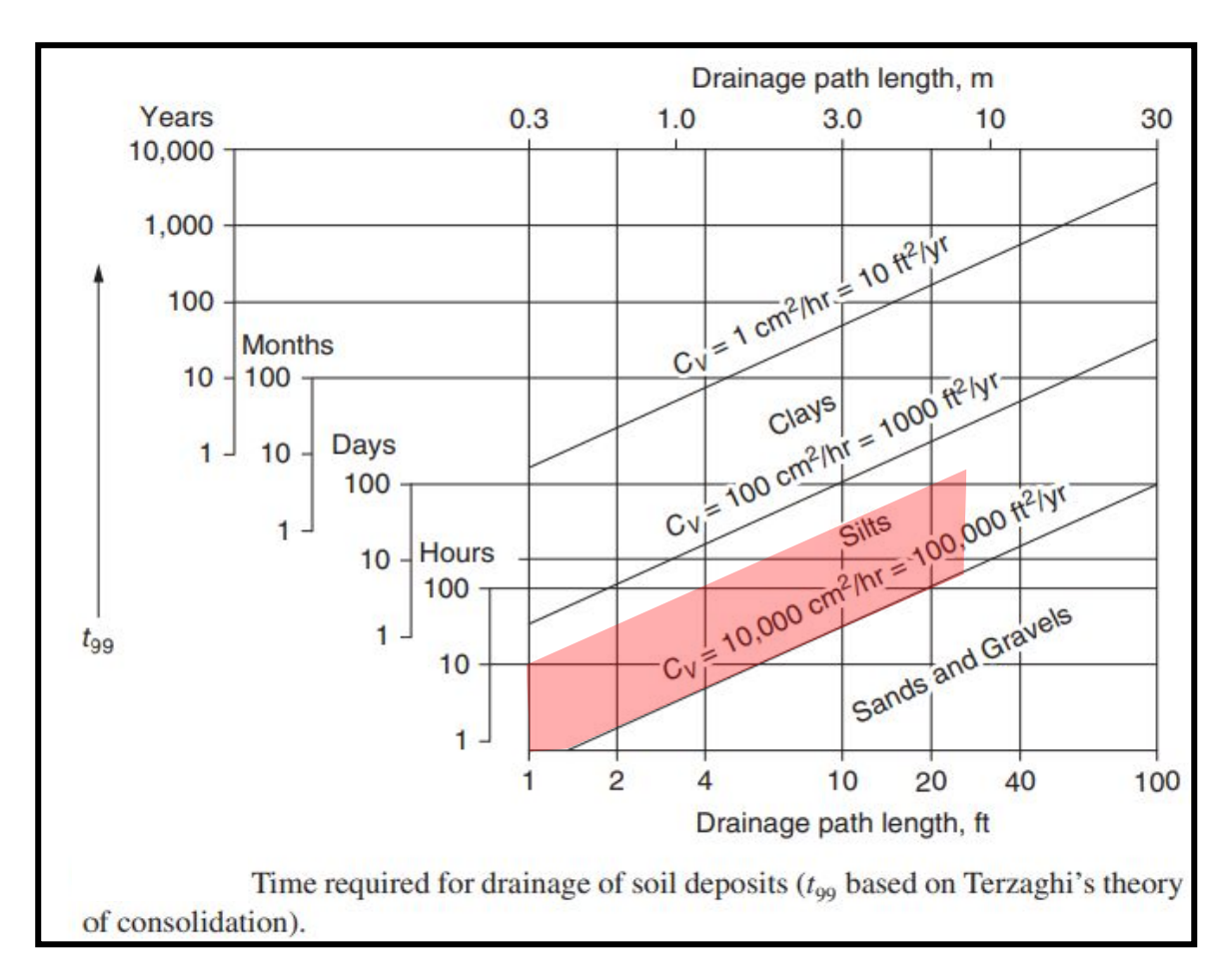
Supplemental Figure S8: Median grain size (μ m), dry bulk density (g/cm³) and loss-onignition % for all Rampal_out_ cores; all Rampal_out_ cores were vibracores. Horizontal error bars for dry bulk density and loss-on-ignition are standard error for all samples within a core, while the vertical error bars are fixed at 5 cm as the samples were collected in 10 cm intervals. There was no discernible relationship between median grain size and depth for the 3 cores, and the predominant grain size is silt. The average LOI for the three cores was 4.2%, with Rampal_out_2,3 both having higher subsamples at depths of 90-100 cm (12.4% organic matter) and 10-20 cm (11.2% organic matter), respectively. The bulk densities ranged from 1.1 to 1.8 g/cm³, with Rampal_out_2 having the most pronounced increase of bulk density with depth.



Supplemental Figure S9: Median grain size (μ m), dry bulk density (g/cm^3) and loss-onignition % for all Rampal_in_ cores. Horizontal error bars for dry bulk density and loss-onignition are standard error for all samples within a core, while the vertical error bars are fixed at 10 cm as the samples were collected in 20 cm intervals. There is no discernible relationship between median grain size and depth, and the predominant grain size is silt. LOI % values were all relatively low (<7.5%), indicating low organic matter, and the bulk densities ranged from 0.9 to 1.8 g/cm³.

4) Dredge Spoil Consolidation and Compaction

After excavation, dredge spoils are deposited alongside the channel margins, unmoved for years (Fig. 2). Thus, there is sufficient time for the sediment to dewater (consolidate) before being used in construction (Fig. S10; Duncan, Wright and Brandon, 2014). Housing plinths constructed in Bangladesh are manually compacted – no heavy machinery is used in the process. Therefore, it can be inferred that the maximum compaction of sediment will not exceed the natural consolidation of the sediment – a 1:1 ratio for bulk densities. However, for conservative estimates, we assume that the maximum amount of compaction, if it exceeds the 1:1 ratio, will not exceed 20%. Thus, the "compaction factor" used in our calculation is 1.2x.



Supplemental Figure S10: Modified from Duncan et al. (2014): All cores extracted in this study were silt-dominated, with <25% clay content except for one 20 cm thick deposit at depth (>2.5 m) that had >25% clay content in Rampal_out_3. The drainage path length, which is strictly in the +y direction, is at its greatest at the apex of the dredge spoil "artificial levees". Assuming a maximum height of 8 meter, the dredge spoils undergo dewatering, or primary consolidation, within a matter of days (as shown by the red shading).

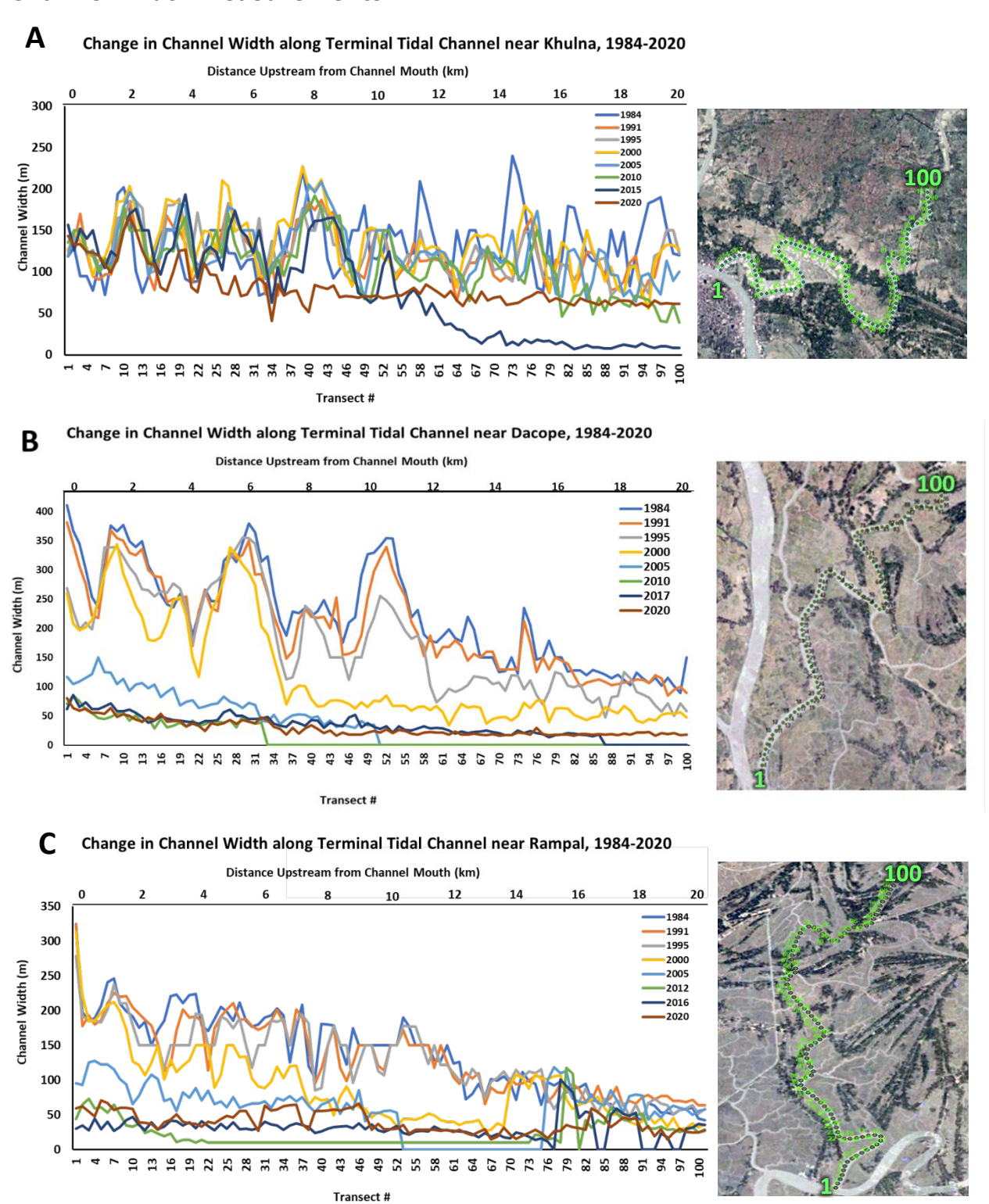
Volumetric (m³) Estimates for Constructing Housing Plinths and Augmenting Existing Embankments

	Volume (m³) for 1 plinth (dimensions 7.5 m x 7.5 m x 1.5 m)	Total # of plinths that can be built with 1.70 x 10 ⁶ m ³	Volume (m³) to elevate 1 km length of embankment (dimensions detailed in Fig. 10B)	Total length (km) of Embankments Elevated with 1.70 x 10 ⁶ m ³
Secondary Compaction 1:1	7.5 m x 7.5 m x 1.5 m = 84.375 m ³	(1.70 x 10 ⁶ m ³)/ 84.375 m ³ = 20, 148 plinths	Area of 6.8 m height embankment – Area of 3.8 m height embankment = 92.4 m ² 92.4 m ² x 1000 m = 92,400 m ³	(1.70 x 10 ⁶ m ³)/ 92,400 m ³ = 18.4 km
Secondary Compaction 1:1.2	84.375 m ³ x 1.2 = 101.25 m ³	(1.70 x 10 ⁶ m ³)/ 101.25 m ³ = 16, 790 plinths	92,400 m ³ x 1.2 = 110,880 m ³	(1.70 x 10 ⁶ m ³)/110,880 m ³ = 15.3 km

Supplemental Table S1: Calculations for how many housing plinths or km-lengths of augmented embankments could be constructed using the dredge spoils $(1.70 \times 10^6 \text{ m}^3)$. For each repurposing idea (plinths vs augmented embankments), there are two calculations – one assuming no secondary compaction and one assuming a secondary compaction of 20% (factor of 1.2), For the embankment dimensions, see Fig. 10, which is modified from Dasgupta et al., (2010).

5) Channel Infilling Analyses and Geometric Calculations

Channel Width Measurements



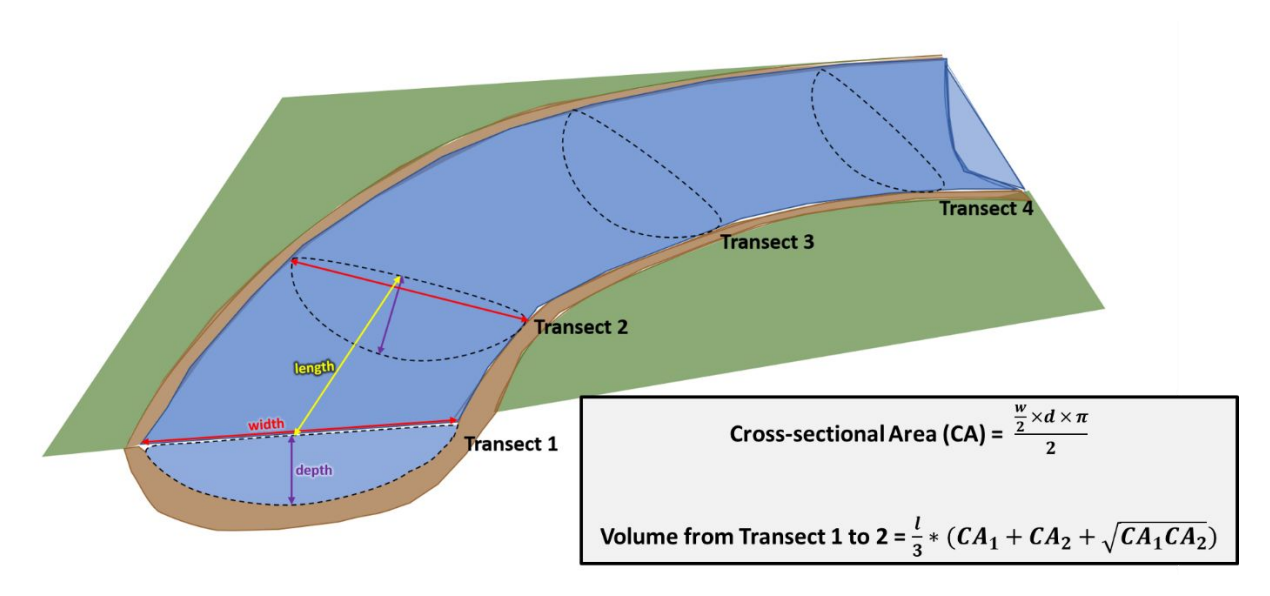
Supplemental Figure S11: Channel width measured along transects 1-100 for Khulna (A), Dacope (B), and Rampal (C) tidal channels. For all three sites, channel width decreases over time, with the largest average decrease at Dacope (B). All graphs are accompanied by 2019 Google Earth images of the sites, showing the three channels and associated transects.

Figure S11A, displays the change in channel width for each transect along the Khulna tidal channel during individual years 1984, 1991, 1995, 2000, 2005, 2010, 2014, and 2020. In general, average channel width decreased most notably in the upstream reaches. For example, transects 50-100 from years 2000 to 2015 decreased in width from 118 to 29 m (a 75% decrease), and transects 25-50 between years 2015 to 2020 decreased in width from 122 to 75 m (a 39% decrease). Then, dredging operations for transects 50-100 were evident, as observed as an increase in average channel width between 2015 and 2020 from 28 to 68 m.

Figure S11B, displays the change in channel width for the transects near Dacope during individual years 1984, 1991, 1995, 2000, 2005, 2010, 2017, and 2020. The upstream reaches (transects 40-100) experienced large channel width reductions starting in 2000 (from an average channel width of 60 m in 2000 to <10 m in 2010, >83% decrease), and the transects closer to the mouth (transects 1-40) experienced large channel width reductions in 2005 (from an average channel width of 83 m in 2005 to 36 m in 2010, 57% decrease). Ultimately, dredging was started after 2010 and completed in 2017 (transects 1-86) and 2020 (transects 87-100). For transects 1-86, the average channel width pre-dredging in 2010 was 17 m

and post-dredging in 2017 was 37 m. For transects 87-100, the average channel width pre-dredging in 2017 was <10 m and post-dredging in 2020 was 19 m. However, for transects 1-86, the channels began infilling post-dredging as the average channel width decreased from 37 m in 2017 to 31 m in 2020 – a 16% decrease in just 3 years.

Figure S11C, depicts the channel width changes for the channel near Rampal for individual years 1984, 1991, 1995, 2000, 2005, 2012, 2016, and 2020. Once again, the upstream channel reaches (transects 49-100) experienced a greater change in channel widths, with the largest changes evident from 1995 to 2000. While the lower reaches (transects 1-48) also decreased during this time (from an average width of 166 to 125 m, 25% decrease), the upper reaches (transects 49-100) experienced significantly more infilling, decreasing from an average width of 93 to 55 m, a decrease of 41%. After 2005, transects 70-100 were cut off from the lower transects by a small, earthen dam constructed by locals. Dredging operations for transects 1-69 started after 2012 and ended in 2016, and average channel width increased from 18 to 31 m. Additional dredging started after 2018 and was still ongoing for transects 1-48 during May 2020 as evidenced by Copernicus imagery. Between 2016 and 2020, the average channel width for transects 1-48 increased from 34 to 50 m.



Supplemental Figure S12: A schematic of a tidal channel, with equally spaced transects denoted by dashed lines. A reducing tidal prism and velocities are causing the channel banks and beds to infill. The formulas for calculating the channel volumes are given.

References for Supplemental Material

Amin, C. M. T. et al. (2015) 'Analysis of Spatial Variation of Groundwater Depths Using Geostatistical Modeling in the vicinity of Sylhet City, Bangladesh'.

Auerbach, L. W. *et al.* (2015) 'Flood risk of natural and embanked landscapes on the Ganges-Brahmaputra tidal delta plain', *Nature Climate Change*, 5(2), pp. 153–157. doi: 10.1038/nclimate2472.

Choudhury, N. Y., Paul, A. and Paul, B. K. (2004) 'Impact of costal embankment on the flash flood in Bangladesh: A case study', *Applied Geography*, 24(3), pp. 241–258. doi: 10.1016/j.apgeog.2004.04.001.

Dasgupta, S. et al. (2010) 'Vulnerability of Bangladesh to Cyclones in a Changing Climate: Potential Damages and Adaptation Cost', World Bank Policy Research Working Paper, (5280).

Duncan, J. M., Wright, S. G. and Brandon, T. L. (2014) 'Soil Strength and Slope Stability, 2nd Edition', *John Wiley & Sons*, p. 336.

EGIS (2000) Environmental Baseline of Gorai River Restoration Project, EGIS II.

Hussain, S. M. and Hoque, M. S. (2020) 'Climate Exodus: The Migration Catastrophe of Bangladesh', 2020 IEEE Region 10 Symposium, TENSYMP 2020, (June), pp. 1185–1188. doi: 10.1109/TENSYMP50017.2020.9231036.

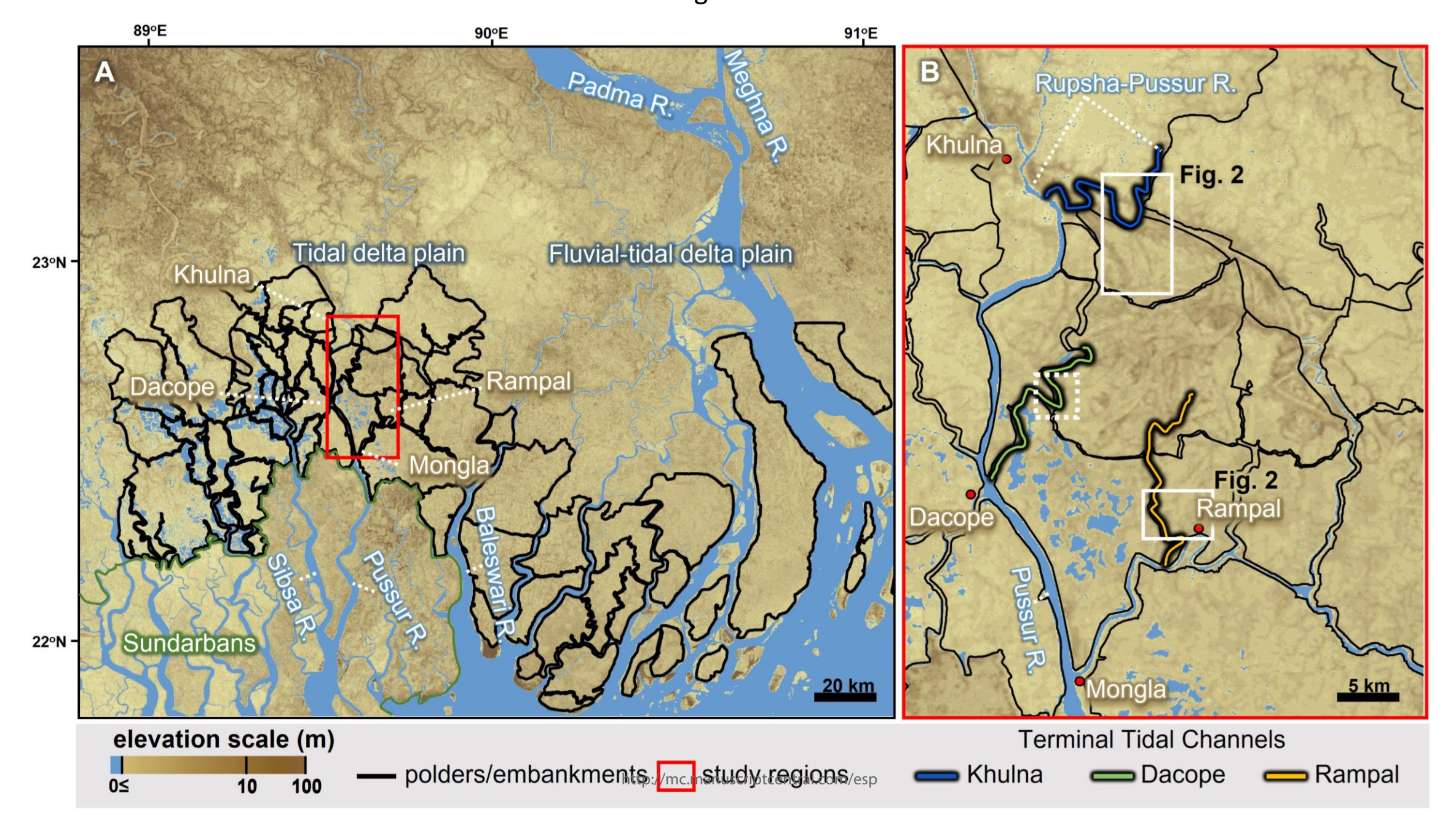
Islam, M. M., Hofstra, N. and Sokolova, E. (2018) 'Modelling the present and futurewater level and discharge of the tidal betna river', *Geosciences* (Switzerland), 8(8), pp. 1–15. doi: 10.3390/geosciences8080271.

Jakobsen, F. et al. (2006) 'Cyclone Storm Surge Levels Along the Bangladeshi Coastline in 1876 and 1960–2000', Coastal Engineering Journal, 48(3), pp. 295–307. doi: 10.1142/S057856340600143X.

Mondal, M. A. M. and Bangladesh Inland Water Transport Authority (2001) Sea Level Rise along the Coast of Bangladesh. Dhaka, Bangladesh.

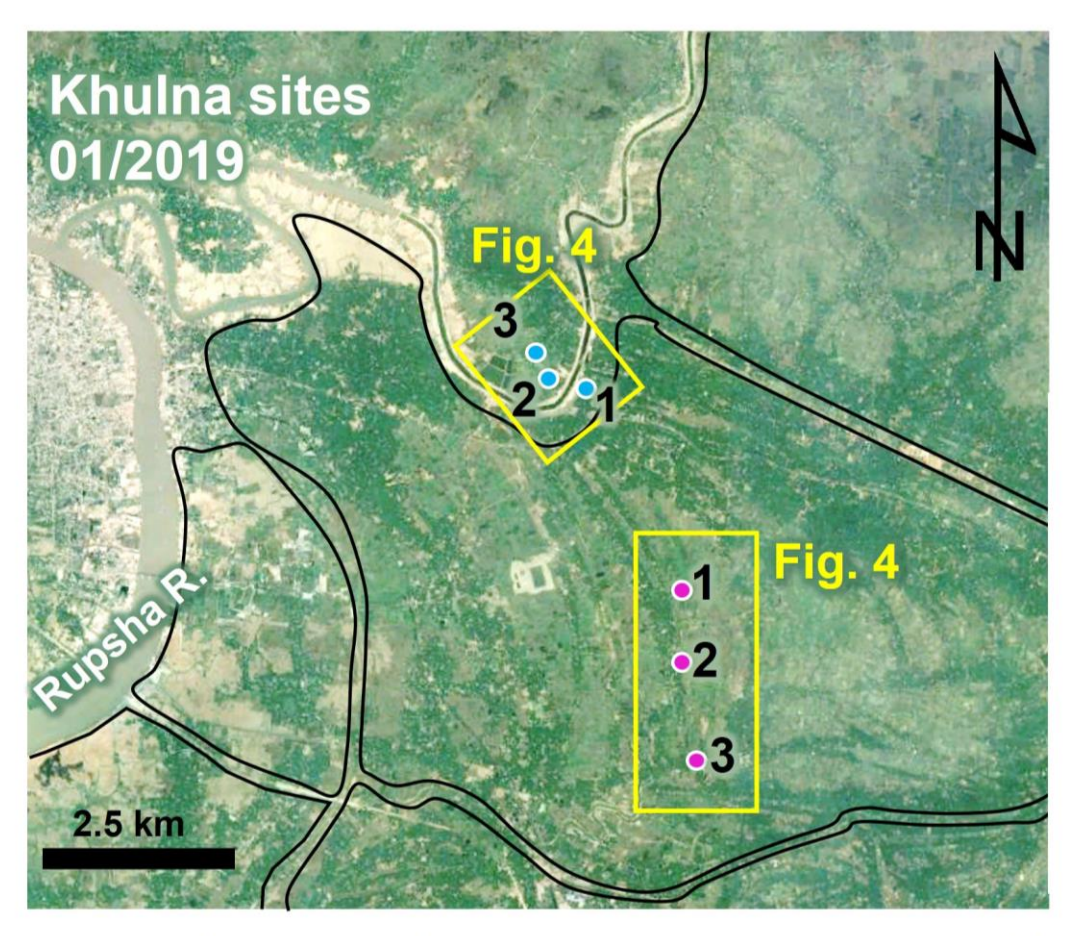
Pethick, J. and Orford, J. D. (2013) 'Rapid rise in effective sea-level in southwest Bangladesh: Its causes and contemporary rates', *Global and Planetary Change*, 111(October), pp. 237–245. doi: 10.1016/j.gloplacha.2013.09.019.

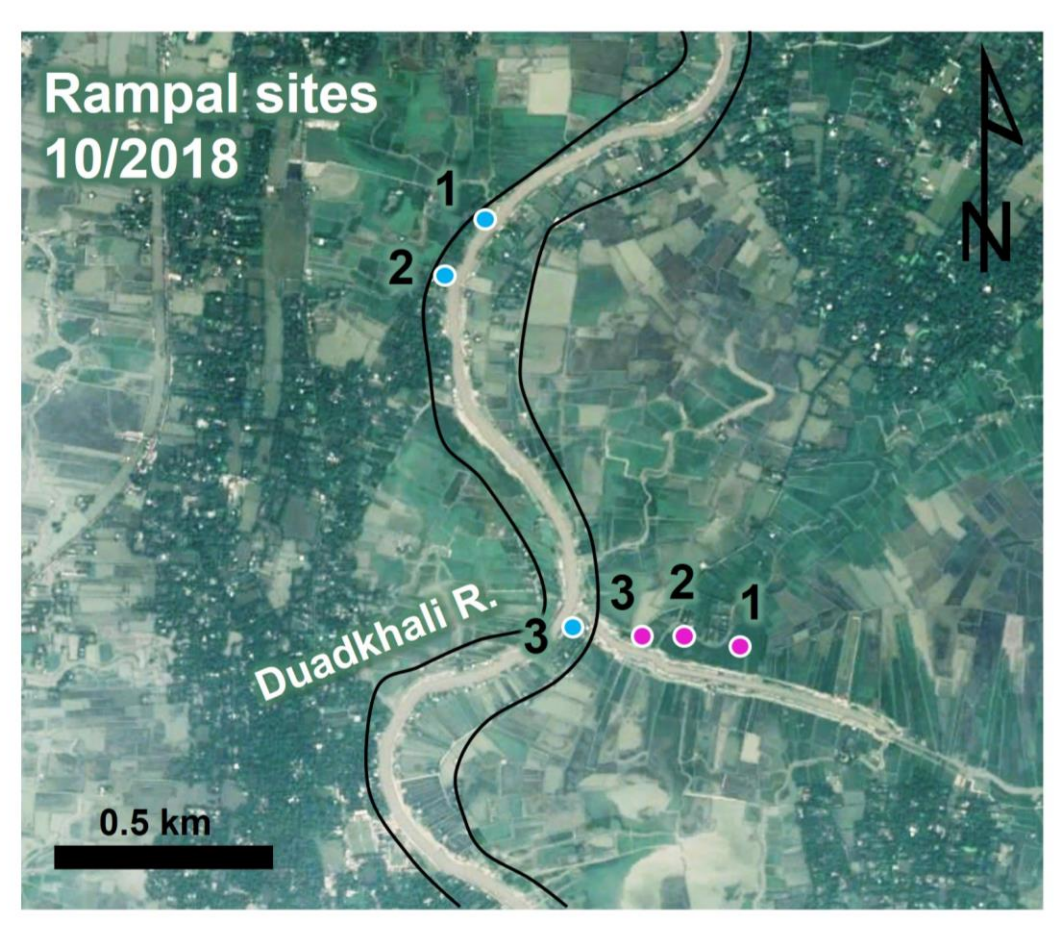
Wilson, C. et al. (2017) 'Widespread infilling of tidal channels and navigable waterways in the human-modified tidal deltaplain of southwest Bangladesh', *Elementa*, 5. doi: 10.1525/elementa.263.









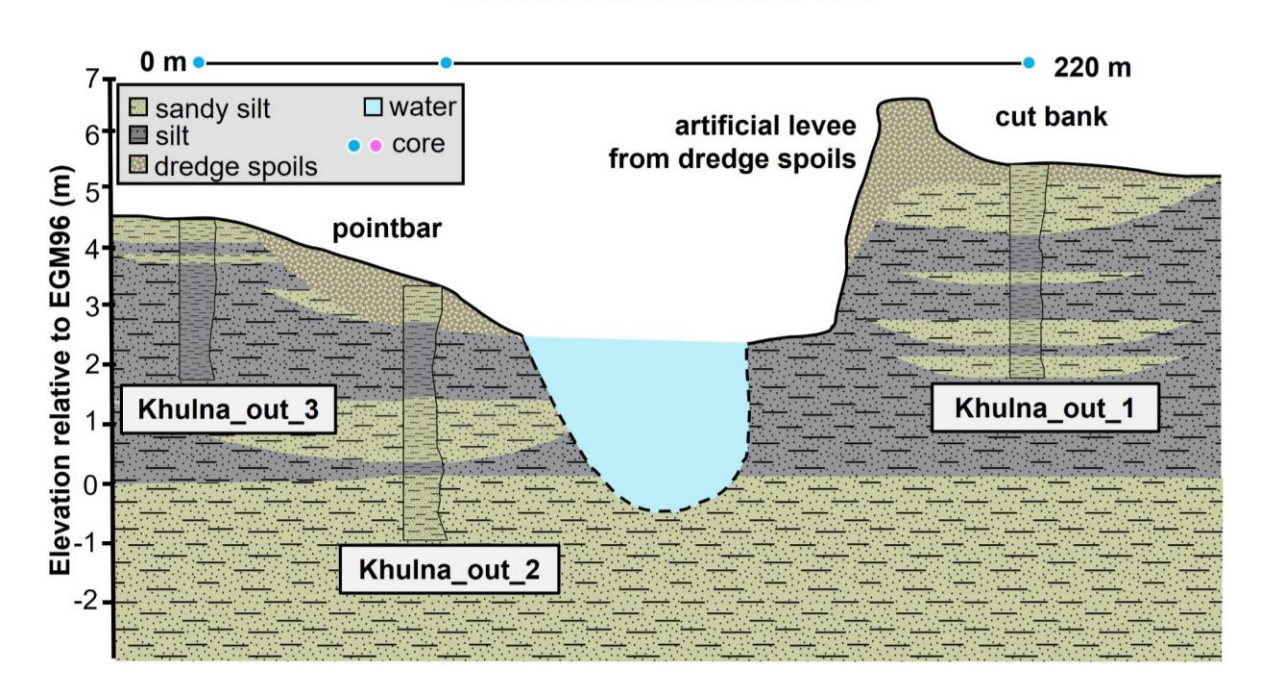


— polders/embankments

core outside embankment

core inside embankment

Unembanked Khulna Site



Embanked Khulna Site



